In the Claims:

Please amend claims 23, 32 and 33 as noted on the attached sheet of paper. As required by 37 C.F.R. § 1.121(c), the amended claims are rewritten with all changes included. In addition, as permitted under 37 C.F.R. § 1.121(c)(3), a clean version of all of the pending claims is submitted as a single amendment paper, which is attached to this response. Also attached is the compare copy of the claims, marked to show all of the changes relative to the previous version of the claims.

REMARKS

Claims 1-20 and 23-33 are pending in the application. Claims 23, 32, and 33 have been amended herein to correct antecedent basis. Accordingly, no new matter has been added by these amendments.

Applicant assumes that all rejections not repeated in the Office Action of June 3, 2002, have been overcome and are withdrawn.

The outstanding rejections are addressed individually below.

1. ***The Amendment filed March 18, 2002 does not contain new matter.***

The Amendment filed March 18, 2002 is objected to under 35 U.S.C. § 132 because it allegedly contains new matter. Applicant respectfully traverses this objection.

M.P.E.P. § 608.04 states that "[i]n establishing a disclosure, applicant may rely not only on the specification and drawing as filed but also on the original claims if their content justifies it. (citation omitted) (emphasis added)

Changing "Oligo 164" to "Oligo 165" at page 58, line 28 is an obvious change in light of the information contained in Table 1 of the specification. Table 1 indicates that Oligo 165 is a hybrid oligonucleotide which is SEQ ID NO: 4.

Similarly, changing SEQ ID NO: 3 to SEQ ID NO: 5 at page 59, line 18 is an obvious change in light of the information contained in Table 1 of the specification, which indicates that oligonucleotide 168 is SEQ ID NO: 5.

Accordingly, as this information was presented correctly in Table I, these changes do not introduce new matter.

Furthermore, the figure to which the discussion at page 58, line 25 to page 59, line 20 refers (FIG. 1) has not been changed. Applicant is merely amending the discussion to correspond more accurately to this figure. Accordingly, no new matter is being added by these amendments.

With regard to the amendment at page 58, line 30, the unamended specification at page 58, line 30 refers to Oligo 190, SEQ ID NO:1. However, there is no Oligo 190 in FIG. 1. According to Table 1, SEQ ID NO: 1 corresponds to Oligo 164. Furthermore, this corresponds to the discussion at page 59, lines 10-15, which states that "the size of the tumor in the animal treated with the inverted hybrid oligonucleotide 166 having SEQ ID NO: 6 was surprisingly smaller from three days after injection onward than the phosphorothioate oligonucleotide 164 having SEQ ID NO: 1." Amended Table 1 refers to SEQ ID NO: 1 as "Antisense."

Accordingly, as this information was presented correctly in FIG. 1, Table 1, and the rest of the paragraph, these changes do not introduce new matter.

The remaining changes in this paragraph merely correct punctuation.

Therefore, Applicant submits that the changes to the paragraph at page 58, line 25 to page 59, line 20 do not add new matter but merely bring the description of the oligonucleotides used into conformance with FIG. 1, Table 1, and the rest of the paragraph.

Accordingly, Applicant respectfully requests that the Examiner reconsider and withdraw this objection.

2. Claims 1-20 and 23-33 are enabled by the specification as filed.

Claims 1-20 and 23-33 stand rejected under 35 U.S.C. § 112, first paragraph, as not being enabled by the specification as filed. Applicant respectfully traverses this rejection.

Claim 1 is directed to a method for inhibiting proliferation of cancer cells comprising administering to the cells a first agent comprising a synthetic, modified oligonucleotide complementary to, and which down-regulates the expression of, nucleic acid encoding protein kinase A subunit RIα, the modified oligonucleotide having from about 15 to about 30 nucleotides and being a hybrid, inverted hybrid, or inverted chimeric oligonucleotide of specific characteristics, and administering to the cells a second agent comprising an antibody that binds to EGFR or a cytotoxic agent selected from an enumerated group, wherein the administering steps may be performed simultaneously or sequentially in any order. Other independent claims are further directed to a pharmaceutical composition and a method for treating cancer.

The Office Action states that the specification, while being enabling for inhibiting proliferation of cancer cells *in vitro*, and in a mouse model comprising administration of HYB 165, does not reasonably provide enablement for treatment of cancer in a patient *in vivo*, and that the specification does not enable a person skilled in the art to which it pertains to use the invention commensurate in scope with these claims. Applicant maintains that the specification does enable the pending claims.

M.P.E.P § 2164.01 states that 35 U.S.C. § 112, first paragraph, "has been interpreted to require that the claimed invention be enabled so that any person skilled in the art can make and use the invention without undue experimentation." (citation omitted) The same section further states that "[t]he fact that experimentation may be complex does not necessarily make it undue, if the art typically engages in such experimentation."

The specification teaches one of skill in the art to how to make the invention (*see, e.g.*, the specification at page 23, line 11 to page 24, line 2, and Example 1 at page 35, line 7 to page 36, line 23).

Furthermore, the specification teaches one of skill in the art how to use the invention (*see, e.g.*, the specification at page 25, lines 16-29 (describing carriers), at page 27, line 15 to page 28, line 14, and page 29, line 8 to page 30, line 10 (describing dosages for the two agents), and page 30, line 24 to page 31, line 22 (describing ways to administer the agents)).

Therefore, the specification has fully enabled the invention as claimed because it teaches how to make and use the invention without undue experimentation.

Furthermore, the specification provides examples indicating that the invention works as claimed.

The oligonucleotides of the invention have been tested *in vitro* in a variety of cell types, both with and without the second agent. The specification indicates that *in vitro* experiments were performed analyzing, *inter alia*, the effect of inverted hybrid or inverted chimeric structure on oligonucleotide-mediated mitogenicity (page 50, line 16 to page 52, line 6) and to determine the ability of inverted hybrid oligonucleotides and inverted chimeric oligonucleotides to activate RNase H *in vitro* when bound to a complementary RNA molecule (page 56, line 4 to page 57, line 28). Furthermore, Examples 13-26 (pages 63-89) describe *in vitro* experiments using oligonucleotides of the invention, both with and without the second agent.

The Office Action states that Applicant allegedly "has not addressed the various factors that contribute to the unpredictable behaviour of antisense compounds in different cellular environments, as described by Crooke (1998)". However, Examples 13-26 (pages 63-89) describe *in vitro* experiments using oligonucleotides of the invention, both with and without the second agent, in a variety of different cellular environments including ZR-75-1 human breast cancer cells, GEO human colon cancer

cells, 1AP, 1A9PTX22 and 1A9PTX10 human ovarian cancer cells, and OVCAR human ovarian cancer cells.

Additionally, although the Office Action cites Crooke (1998) for the fact that one cannot predict *in vivo* pharmacokinetics of the compounds based on *in vitro* studies, the claimed invention has in fact been tested and found to work *in vivo*. Examples 27, 28, and 29 (pages 90-95) as well as Figures 16, 17, and 18 of the instant patent application provide examples and data indicating that the claimed invention does work *in vivo* in an accepted animal model. More specifically, Example 27 indicates that HYB 165 inhibits tumor growth after intraperitoneal or oral administration in mice. The data for this experiment is presented in Figures 16A and 16B. Example 28 indicates that oral HYB 165 cooperatively inhibits tumor growth and increases survival in combination with taxol. Data for this experiment is presented in Figures 17A and 17B. Example 29 indicates that the cooperative antitumor effect of HYB 165 with taxol is accompanied by inhibition of new vessel formation and growth factor production as well as other results of histochemical analysis. Data for this experiment is presented in the table in Figure 18. Additional support for the *in vivo* use of the methods and pharmaceutical compositions of the invention is found in the description of the figures in the specification at page 20, lines 9-29.

Additionally, Example 10 indicates that a single dose of RIα antisense, hybrid, or inverted hybrid oligonucleotide was tested by injection into the right flank of athymic mice previously innoculated with tumor cells and tumor volumes were obtained (page 58, line 25 to page 59, line 20) and the results are shown in Figure 1. Thus, several oligonucleotides of the invention were tested *in vivo*.

Furthermore, Tortora *et al.*, (1997) *Proc. Natl. Acad. Sci. USA* **94:**12586-12591, which is attached hereto as Appendix A, was previously cited by the Examiner and referred to in the Rule 132 Declaration filed March 26, 2001. This reference indicates that HYB 190, an inverted chimeric oligonucleotide, combined with paclitaxel, significantly increased tumor growth inhibition as compared to untreated mice or to mice treated with each single agent. This reference was cited by the Examiner under 35

USC § 102(a), and therefore must have been considered by the Examiner to show enablement.

Thus, hybrid, inverted hybrid, and inverted chimeric oligonucleotides have been shown to work *in vivo*. Furthermore, the hybrid and inverted chimeric oligonucleotides have been shown to work cooperatively with a second agent according to the invention.

Applicant has shown successful correlation between *in vitro* and *in vivo* studies in Examples 27, 28, and 29, as well as in Example 10 with the use of protein kinase A subunit RIα specific oligonucleotides in an established, art accepted mouse model These results and the art at the time of filing suggest that *in vitro* results are predictive of *in vivo* use for inhibiting proliferation of cancer cells and that the oligonucleotides of the invention work *in vivo*.

Furthermore, Crooke (1998) cited by the Examiner, states that "Overall, the behavior of phosphorothioates in the plasma of humans appears to be similar to that in other species." (Page 18) Crooke (1998) further states that a "relatively large number of reports of in vivo activities of phosphorothioate oligonucleotides have now appeared documenting activities both after local and systemic administration" (citation omitted) (page 22), and provides Table 1 indicating reported activity of antisense oligonucleotides in animal models including the rat, mouse, rabbit, chicken, and duck (pages 23-24).

The Office Action alleges that Applicant has "not provided a clear nexus between the use of the HYB 165 oligonucleotide, particularly in a mouse model, and the use of all oligonucleotides encompassed by the methods of the claimed invention, specifically in organisms other than the mouse." (Office Action, page 6) Applicant disagrees with this statement.

Applicant respectfully submits that the evidence provided above indicates a nexus between the use of the HYB 165 oligonucleotide in a mouse model (as well as the use of HYB 166 in a mouse model) and the use of the oligonucleotides complementary to, and which down-regulate the expression of, nucleic acid encoding protein kinase A

subunit RIα as claimed. In addition, mouse models have been used as acceptable animal models for cancer treatment for years. In fact, one of skill in the art would be aware that mouse models are the "standard" animal model for taking a drug into a clinical setting, including for cancer treatment.

Furthermore, Applicant notes that claims 1-20 relate to a method for inhibiting proliferation of cancer cells and to a pharmaceutical composition, as compared to claims 23-33 which relate to a method for treating cancer in an afflicted subject.

The claims of the present invention are limited to oligonucleotides complementary to, and which down-regulate the expression of, nucleic acid specifically encoding protein kinase A subunit RIα. The specification indicates that at the time of the invention the "sequence of this gene [was] known. Thus, an oligonucleotide of the invention can have any nucleotide sequence complementary to any region of the gene." (Specification at page 21, lines 22-25). It is known in the art that scanning arrays can be used to facilitate synthesis of antisense oligonucleotides. Milner et al. (*Nature Biotechnology* (1997) **15**:537-541; attached hereto as Appendix B) demonstrates "a combinatorial technique that allows simultaneous assessment of all possible ONs [oligonucleotides] within a given region identifying sequences open to duplex formation. An oligonucleotide 'scanning' array reduces the number of synthesis steps while providing a parallel and exhaustive analysis of all ONs in the region to be targeted." (page 537) This article further states that "those ONs which give high duplex yield on the array proved to be effective antisense agents in in vitro RNase H and translation studies." (page 537) As stated in the abstract, "the arrays provide a simple empirical method of selecting effective antisense oligonucleotides for any RNA target of known sequence."

Although the Office Action questions the usefulness of gene arrays, Applicant respectfully submits that those with skill in the art do find gene arrays useful. As an example, Applicant encloses herewith a paper by Cho, *et al.*, (2001) *PNAS* **98**(17): 9819-9823 (attached hereto as Appendix C), which shows the use of DNA microarrays to

conduct a systematic characterization of gene expression in cells exposed to antisense, either exogenously or endogenously. (*See* abstract)

Furthermore, even if this statement were true, it does not present a problem for enablement purposes. First, as noted above, M.P.E.P § 2164.01 states that "[t]he fact that experimentation may be complex does not necessarily make it undue, if the art typically engages in such experimentation." Second, even if some of the species in a genus claim are inoperative, the claims are not necessarily invalid. *Atlas Powder Co. v. E.I. Du Pont de Nemours & Co.*, 750 F.2d 1569, 1576; 224 U.S.P.Q. (BNA) 409. "It is not a function of the claims to specifically exclude...possible inoperative substances...." *Id. (citing In re Dinh-Nguyen*, 492 F.2d 856, 858-59, 181 U.S.P.Q. (BNA) 46, 48 (CCPA 1974) (emphasis omitted); *accord, In re Geerdes*, 491 F.2d 1260, 1265, 180 U.S.P.Q. (BNA) 789, 793 (CCPA 1974); *In re Anderson*, 471 F.2d 1237, 1242, 176 U.S.P.Q. (BNA) 331, 334-35 (CCPA 1973)).

Applicant respectfully asserts the Examiner may be confusing the requirements under law for obtaining a patent with the requirements for obtaining government approval for marketing a particular drug for human consumption. *See In re Brana*, 51 F.3d 1560, 1567, 34 U.S.P.Q.2d (BNA) 1436 (Fed. Cir. 1995), citing *Scott v. Finney*, 34 F.3d 1058, 1063, 32 U.S.P.Q.2d (BNA) 115, 120 (Fed. Cir. 1994) ("Testing for the full safety and effectiveness of a prosthetic device is more properly left to the Food and Drug Administration (FDA). Title 35 does not demand that such human testing occur within the confines of Patent and Trademark Office (PTO) Proceedings"). Determining effective parameters for the administration to cancer cells of a first agent comprising a synthetic, modified oligonucleotide complementary to, and which down-regulates the expression of, nucleic acid encoding protein kinase A subunit RIα, the modified oligonucleotide having from about 15 to about 30 nucleotides and being a hybrid, inverted hybrid, or inverted chimeric oligonucleotide of specific characteristics, and a second agent comprising an antibody that binds to EGFR or a cytotoxic agent selected from an enumerated group, and determining the therapeutically effective amount required for the treatment would be considered a routine process by skilled artisans, and would not require undue experimentation.

Thus, Applicant respectfully asserts that the Examiner's concerns regarding *in vivo* use are inappropriate.

Additionally, Applicant notes that the Office Action discusses the language "consisting essentially of" in the context of a 35 U.S.C. § 112, first paragraph, enablement rejection. It is unclear to Applicant whether these claims are also being rejected under 35 U.S.C. § 112, second paragraph. Applicant assumes that unless otherwise explicitly indicated these claims stand rejected only under 35 U.S.C. § 112, first paragraph.

Therefore, Applicant submits that in view of the foregoing remarks and the references submitted, pending claims 1-20 and 23-33 are enabled by the specification as filed.

Accordingly, Applicant respectfully requests that the rejection of these claims under 35 U.S.C. § 112, first paragraph, be reconsidered and withdrawn.

CONCLUSIONS

In view of the arguments set forth above, Applicant respectfully submits that the rejections contained in the final Office Action mailed on June 3, 2002, have been overcome, and that the claims are in condition for allowance. If the Examiner believes that any further discussion of this communication would be helpful, she is invited to contact the undersigned at the telephone number provided below.

Applicant encloses herewith a Petition for a Two Month Extension of Time pursuant to 37 C.F.R. § 1.136 up to and including November 4, 2002 (November 3, 2002 being a Sunday), to respond to the Examiner's Office Action mailed on June 3, 2002. Please charge deposit account no. 08-0219 the $200.00 fee for this purpose.

Applicant also encloses herewith a Supplemental Information Disclosure Statement. Please charge Deposit Account No. 08-0219 the $180.00 fee for this submission.

No other fees are believed to be due in connection with this response. However, please charge any underpayments or credit any overpayments to Deposit Account No. 08-0219.

Respectfully submitted,

Ann-Louise Kerner, Ph.D.
Reg. No. 33,523

November 4, 2001

HALE AND DORR LLP
60 State Street
Boston, MA 02109
Tel: (617) 526-6000
Fax: (617) 526-5000

Attachments: Clean Copy of Pending Claims
Compare Copy of Claims

Compare Copy of Pending Claims
U.S.S.N. 09/412,947
Filed October 5, 1999
November 4, 2002

1. (*Once Amended*) A method for inhibiting proliferation of cancer cells comprising

(a) administering to the cells a first agent comprising a synthetic, modified oligonucleotide complementary to, and which down-regulates expression of, nucleic acid encoding protein kinase A subunit RIα, the modified oligonucleotide having from about 15 to about 30 nucleotides and being a hybrid, inverted hybrid, or inverted chimeric oligonucleotide,

the hybrid oligonucleotide comprising a region of at least two deoxyribonucleotides, flanked by 3' and 5' flanking ribonucleotide regions each having at least four ribonucleotides,

the inverted hybrid oligonucleotide comprising a region of at least four ribonucleotides flanked by 3' and 5' flanking deoxyribonucleotide regions of at least two deoxyribonucleotides,

and the inverted chimeric oligonucleotide comprising an oligonucleotide nonionic region of at least four nucleotides flanked by two oligonucleotide phosphorothioate regions; and

(b) administering to the cells a second agent comprising an antibody that binds to epidermal growth factor receptor (EGFR) or a cytotoxic agent selected from the group consisting of taxanes, platinum-derived agents, and topoisomerase II-selective drugs;

wherein the administering steps may be performed simultaneously or sequentially in any order.

2. The method of claim 1, wherein the oligonucleotide is a hybrid oligonucleotide.

3. The method of claim 1, wherein the oligonucleotide has a nucleotide sequence consisting essentially of the nucleotide sequence set forth in SEQ ID NO:4.

4. The method of claim 1, wherein the second agent is an antibody that binds to EGFR.

5. The method of claim 4, wherein the antibody is a monoclonal antibody.

6. The method of claim 5, wherein the antibody is C225.

7. The method of claim 1, wherein the second agent is a taxane.

8. The method of claim 7, wherein the taxane is selected from the group consisting of paclitaxel and docetaxel.

9. The method of claim 1, wherein the second agent is administered prior to administration of the first agent.

10. The method of claim 1, wherein the cancer cells are human cancer cells.

11. The method of claim 10, wherein the human cancer cells are selected from the group consisting of breast cancer cells, colon cancer cells, and ovarian cancer cells.

12. (*Once Amended*) A pharmaceutical composition comprising

(a) a first agent comprising a synthetic, modified oligonucleotide complementary to, and which down-regulates expression of, nucleic acid encoding protein kinase A subunit RIα, the modified oligonucleotide having from about 15 to about 30 nucleotides and being a hybrid, inverted hybrid, or inverted chimeric oligonucleotide,

the hybrid oligonucleotide comprising a region of at least two deoxyribonucleotides, flanked by 3' and 5' flanking ribonucleotide regions each having at least four ribonucleotides,

the inverted hybrid oligonucleotide comprising a region of at least four ribonucleotides flanked by 3' and 5' flanking deoxyribonucleotide regions of at least two deoxyribonucleotides,

and the inverted chimeric oligonucleotide comprising an oligonucleotide nonionic region of at least four nucleotides flanked by two oligonucleotide phosphorothioate regions; and

(b) a second agent comprising an antibody that binds to epidermal growth factor receptor (EGFR) or a cytotoxic agent selected from the group consisting of taxanes, platinum-derived agents, and topoisomerase II-selective drugs.

13. (Once Amended) The pharmaceutical composition of claim 12, wherein the oligonucleotide is a hybrid oligonucleotide.

14. (Once Amended) The pharmaceutical composition of claim 12, wherein the oligonucleotide has a nucleotide sequence consisting essentially of the nucleotide sequence set forth in SEQ ID NO:4.

15. (*Once Amended*) The pharmaceutical composition of claim 12, wherein the second agent is an antibody that binds to EGFR.

16. (*Once Amended*) The pharmaceutical composition of claim 15, wherein the antibody is a monoclonal antibody.

17. (*Once Amended*) The pharmaceutical composition of claim 12, wherein the antibody is C225.

18. (*Once Amended*) The pharmaceutical composition of claim 12, wherein the second agent is a taxane.

19. (*Once Amended*) The pharmaceutical composition of claim 18, wherein the taxane is selected from the group consisting of paclitaxel and docetaxel.

20. (*Once Amended*) The pharmaceutical composition of claim 12, wherein the second agent is administered prior to administration of the first agent.

23. (*Twice Amended*) A method for treating cancer in an afflicted subject comprising

(a) administering to the ~~cells~~**subject** a first agent comprising a synthetic, modified oligonucleotide complementary to, and which down-regulates expression of, nucleic acid encoding protein kinase A subunit RIα, the modified oligonucleotide having from about 15 to about 30 nucleotides and being a hybrid, inverted hybrid, or inverted chimeric oligonucleotide,

the hybrid oligonucleotide comprising a region of at least two deoxyribonucleotides, flanked by 3' and 5' flanking ribonucleotide regions each having at least four ribonucleotides,

the inverted hybrid oligonucleotide comprising a region of at least four ribonucleotides flanked by 3' and 5' flanking deoxyribonucleotide regions of at least two deoxyribonucleotides,

and the inverted chimeric oligonucleotide comprising an oligonucleotide nonionic region of at least four nucleotides flanked by two oligonucleotide phosphorothioate regions; and

(b) administering to the ~~cells~~**subject** a second agent comprising an antibody that binds to epidermal growth factor receptor (EGFR) or a cytotoxic agent selected from the group consisting of taxanes, platinum-derived agents, and topoisomerase II-selective drugs;

wherein the administering steps may be performed simultaneously or sequentially in any order.

24. The method of claim 23, wherein the oligonucleotide is a hybrid oligonucleotide.

25. The method of claim 24, wherein the oligonucleotide has a nucleotide sequence consisting essentially of the nucleotide sequence set forth in SEQ ID NO:4.

26. The method of claim 23, wherein the second agent is an antibody that binds to EGFR.

27. The method of claim 26, wherein the antibody is a monoclonal antibody.

28. The method of claim 27, wherein the antibody is C225.

29. The method of claim 23, wherein the second agent is a taxane.

30. The method of claim 29, wherein the taxane is selected from the group consisting of paclitaxel and docetaxel.

31. The method of claim 23, wherein the second agent is administered prior to administration of the first agent.

32. (*Once Amended*) The method of claim 23, wherein the ~~cancer cells are~~**subject is a** human ~~cancer cells~~.

33. (*Once Amended*) The method of claim 32, wherein the human **has a** cancer ~~cells are~~ selected from the group consisting of breast cancer ~~cells~~, colon cancer ~~cells~~, and ovarian cancer ~~cells~~.

APPENDIX A

Proc. Natl. Acad. Sci. USA
Vol. 94, pp. 12586–12591, November 1997
Medical Sciences

Synergistic inhibition of human cancer cell growth by cytotoxic drugs and mixed backbone antisense oligonucleotide targeting protein kinase A

GIAMPAOLO TORTORA*†, ROSA CAPUTO*, VINCENZO DAMIANO*, ROBERTO BIANCO*, STEFANO PEPE*, A. RAFFAELE BIANCO*, ZHIWEI JIANG‡, SUDHIR AGRAWAL‡, AND FORTUNATO CIARDIELLO*

*Cattedra di Oncologia Medica, Dipartimento di Endocrinologia e Oncologia Molecolare e Clinica, Università Federico II, Via Pansini 5, 80131 Napoli, Italy; and ‡Hybridon, Inc, Cambridge, MA 02139

Communicated by Paul C. Zamecnik, Worcester Foundation for Biomedical Research, Shrewsbury, MA, September 15, 1997 (received for review July 1, 1997)

ABSTRACT **Protein kinase A type I plays a key role in neoplastic transformation, conveying mitogenic signals of different growth factors and oncogenes. Inhibition of protein kinase A type I by antisense oligonucleotides targeting its RIα regulatory subunit results in cancer cell growth inhibition *in vitro* and *in vivo*. A novel mixed backbone oligonucleotide HYB 190 and its mismatched control HYB 239 were tested on soft agar growth of several human cancer cell types. HYB 190 demonstrated a dose-dependent inhibition of colony formation in all cell lines whereas the HYB 239 at the same doses caused a modest or no growth inhibition. A noninhibitory dose of each mixed backbone oligonucleotide was used in OVCAR-3 ovarian and GEO colon cancer cells to study whether any cooperative effect may occur between the antisense and a series of cytotoxic drugs acting by different mechanisms. Treatment with HYB 190 resulted in an additive growth inhibitory effect with several cytotoxic drugs when measured by soft agar colony formation. A synergistic growth inhibition, which correlated with increased apoptosis, was observed when HYB 190 was added to cancer cells treated with taxanes, platinum-based compounds, and topoisomerase II selective drugs. This synergistic effect was also observed in breast cancer cells and was obtained with other related drugs such as docetaxel and carboplatin. Combination of HYB 190 and paclitaxel resulted in an accumulation of cells in late S-G_2 phases of cell cycle and marked induction of apoptosis. A cooperative effect of HYB 190 and paclitaxel was also obtained *in vivo* in nude mice bearing human GEO colon cancer xenografts. These results are the first report of a cooperative growth inhibitory effect obtained in a variety of human cancer cell lines by antisense mixed backbone oligonucleotide targeting protein kinase A type I-mediated mitogenic signals and specific cytotoxic drugs.**

Protein kinase A (PKA), a signal-transducing protein playing a key role in the control of cell growth and differentiation, is present in mammalian cells in two distinct isoforms, type I (PKAI) and type II (PKAII) (1, 2). PKAI is directly involved in cell proliferation and neoplastic transformation (1, 3), is required for the $G_1 > S$ transition of the cell cycle (3), mediates the mitogenic signals of different growth factors including epidermal growth factor and transforming growth factor type α (4–6), and is overexpressed in the majority of human cancers, correlating with worse clinicopathological features and prognosis in ovarian and breast cancer patients (7, 8). Conversely, PKAII is preferentially expressed in normal tissues and seems to be involved in cell growth arrest and differentiation (1, 9, 10). It has been shown that the selective down-regulation of PKAI by the site-selective cAMP analog 8-Cl-cAMP leads to inhibition of cancer cell growth in a wide variety of cancer cell types *in vitro* and *in vivo* (1, 4, 5, 11, 12) and is accompanied by inhibition of expression of different oncogenes and growth factors (1, 4, 5, 11). Several studies have also demonstrated that different antisense oligodeoxynucleotides targeting the RIα subunit of PKAI expression cause cell growth arrest and differentiation in a wide variety of cancer cell lines (13, 14). A recent study has shown that an RIα antisense phosphorothioate oligodeoxynucleotide (PS-oligo) is able to inhibit the growth of human colon cancer xenografts in nude mice (15).

A large number of *in vitro* and *in vivo* studies have demonstrated that PS-oligos complementary to the mRNA of proteins involved in the process of neoplastic transformation and progression are effective in inhibiting cancer cell growth (15–21). However, toxicity studies conducted with PS-oligos in animal models and humans have shown dose-dependent side effects, which may be due to the polyanionic structure of PS-oligos and to mitogenic immune response (22–24). Presently, PS-oligos are being tested for their therapeutic potential in human clinical trials. Although PS-oligos have shown promising results as the first generation of oligonucleotides, to further improve their therapeutic potential we have studied mixed-backbone oligonucleotides (MBOs). MBOs have appropriately placed segments of PS-oligo and segments of modified oligodeoxy- or oligoribonucleotides (24). The MBO that we have used in the present study contains five methylphosphonate linkages in the middle of the PS-oligo. These centrally modified oligonucleotides have shown a significant reduction of side-effects *in vivo* compared with PS-oligos (24).

We have used a MBO targeting the RIα subunit of PKAI, alone or in combination with a series of cytotoxic drugs, to determine its antiproliferative effect *in vitro* and *in vivo* on a variety of human cancer cell lines. We have demonstrated that the RIα antisense MBO inhibits the growth of different human cancer cell lines at submicromolar concentrations and has a synergistic growth inhibitory activity with various classes of cytotoxic drugs, including taxanes, platinum-derived agents, and topoisomerase II-selective drugs. Finally, we have observed in absence of toxicity a cooperative antitumor effect of the antisense with paclitaxel in nude mice.

MATERIALS AND METHODS

Cell Lines. LS 174T and GEO human colon cancer, MDA-MB-231 and MDA-MB-468 human breast cancer and

The publication costs of this article were defrayed in part by page charge payment. This article must therefore be hereby marked "*advertisement*" in accordance with 18 U.S.C. §1734 solely to indicate this fact.

Abbreviations: PS-oligo, phosphorothioate oligodeoxynucleotide; MBO, mixed-backbone oligonucleotides; PKA, protein kinase A.

†To whom reprint requests should be addressed.

OVCAR-3 human ovarian cancer cells were purchased from American Type Culture Collection. Docetaxel was a kind gift of Rhone-Poulenc Rorer (Antony Cedex, France). 5-Fluorouracil, methotrexate, cisplatin, camptothecin, doxorubicin, etoposide, paclitaxel, carboplatin, and vincristine were purchased from Sigma. All drugs were diluted in appropriate solvents and used as ×100 concentrated stock.

MBOs. The two oligonucleotides used in the study are HYB 190, GCGTGC*CTCCT*CACTGGC; [targeted against the N-terminal 8–13 codons of the RIα regulatory subunit of PKA (15)] and HYB 239, GCATGC*ATCCG*CACAGGC. HYB 190 and HYB 239 contain phosphorothioate and methylphosphonate internucleotide linkages. These linkages are identified by normal (phosphorothioate) and bold (methylphosphonate) face type for the nucleosides flanking each position. HYB 239 is a control oligonucleotide and contains four mismatched nucleosides as underlined. The two oligonucleotides have been synthesized by the protocol described earlier (24). The identity and purity of the oligonucleotides was confirmed by [^{31}P]NMR, capillary gel electrophoresis, hybridization melting temperature, and A_{269}/mass ratio.

Cell Growth Experiments and Antisense Treatment. LS 174T, MDA-MB-231, and MDA-MB-468 cell lines were maintained in DMEM. OVCAR-3 cells were grown in a 1:1 mixture of DMEM and Ham's-F12 medium. GEO cells were grown in McCoy medium. All media, purchased from Flow Laboratories, were supplemented with 10% heat inactivated fetal bovine serum/20 mM Hepes, pH 7.4/5 mM glutamine/100 units ml penicillin/100 μg/ml streptomycin (Flow Laboratories). Cells were maintained in a humidified atmosphere of 95% air/5% CO_2 at 37°C. For cell growth experiments in soft agar 10^4 cells/well were seeded in 24 multiwell cluster dishes as described (4) and treated with different concentrations of the indicated cytotoxic drug (day 0). The HYB 190 or HYB 239 antisense RIα MBO were added after 12 h (day 1) and on days 2, 3, and 4. Twelve days after the last treatment, cells were stained with nitroblue tetrazolium (Sigma) and colonies larger than 0.05 mm were counted.

Flow Cytometric Analysis of Cell Cycle by Propidium Iodide Staining. Cells seeded in monolayer in 6-well dish clusters were treated with the indicated cytotoxic drug. After 24 hrs (day 1) either HYB 190 or HYB 239 antisense RIα was added and the treatment was repeated on days 2, 3, and 4. At the indicated time points cells were harvested, fixed in 70% ethanol, stained with a propidium iodide solution (Sigma), and their DNA content was analyzed in duplicate by a FACScan flow-cytometer (Becton Dickinson) coupled with a Hewlett–Packard computer, as described (4). Cell cycle data analysis was performed by the CELL-FIT program (Becton Dickinson) (4).

Apoptosis. Flow cytometric analysis of apoptotic cell death was performed on cell pellet fixed in ethanol 70%, washed in PBS, and mixed with RNase (Sigma) and propidium iodide solution following the method reported (25). DNA content was analyzed by a FACScan flow-cytometer (Becton Dickinson) coupled with a Hewlett–Packard computer, and the percent of apoptotic cells was calculated using the LYSYS software (Becton Dickinson).

***In Vivo* Studies with Antisense in Nude Mice.** Five- to 6-week-old female BALB/c athymic (nu^+/nu^+) mice were purchased from Charles River Breeding Laboratories. The research protocol was approved and mice were maintained in accordance to institutional guidelines of the University of Naples Animal Care and Use Committee. Mice were acclimated to the University of Naples Medical School Animal Facility for 1 week prior to being injected with cancer cells. Mice were injected s.c. with 10^7 GEO cells that had been resuspended in 200 μl of Matrigel (Collaborative Biomedical Products, Bedford, MA). After 10 days, when well established tumors of approximately 0.4 cm^3 in diameter were detected,

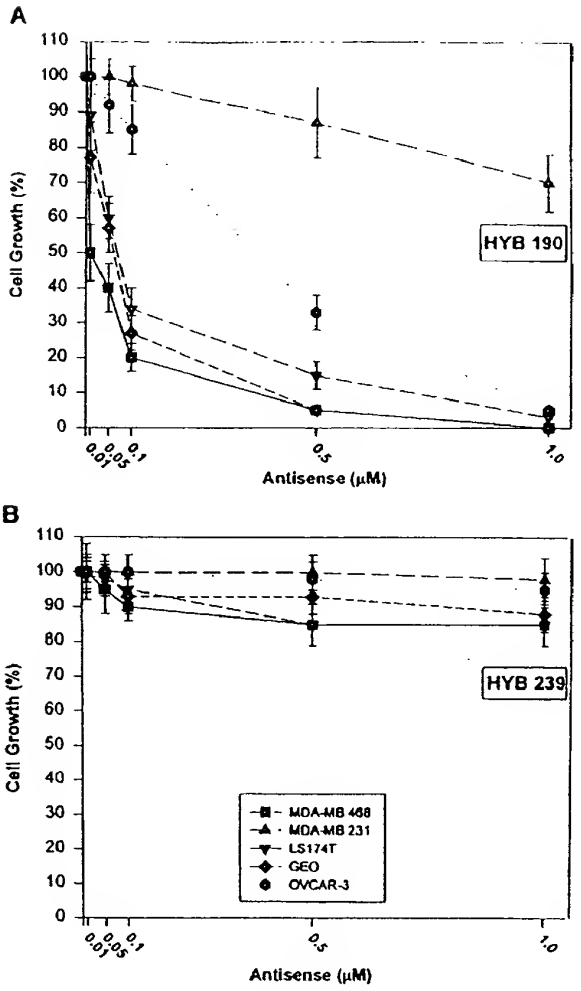

FIG. 1. Dose-dependent effect of the RIα antisense MBO HYB 190 and its control sequence HYB 239 in different cancer cell lines. (*A*) HYB 190. (*B*) HYB 239. Data represent means and standard errors of three different experiments with each performed in triplicate.

seven mice/group were treated i.p. either with paclitaxel (20 mg/kg) (26) (once, on day 1), or with the MBOs HYB 190 (10 mg/kg) or HYB 239 (10 mg/kg) (for 5 days, from day 2 to 6), or with paclitaxel in combination with either HYB 190 or HYB 239 in a sequential schedule; that is, the mice received the cytotoxic drug first (day 1), then, the oligonucleotides were administered for 5 consecutive days (day 2–6). Tumor size was measured twice weekly up to 67 days from tumor cell injection. Tumor size was measured using the formula $\pi/6 \times$ larger diameter $\times$ (smaller diameter)^2, as reported (27).

Statistical Analysis. The Student's *t* test (28) was used to evaluate the statistical significance of the results. All *P* values represent two-sided tests of statistical significance. All analyses were performed with the BMDP NEW SYSTEM statistical package version 1.0 for Microsoft Windows (BMDP Statistical Software, Los Angeles).

RESULTS

Effect of the RIα Antisense MBO in Cancer Cells. HYB 190, an 18-mer MBO antisense to the N-terminal 8–13 codons of the RIα subunit of PKAI, and the control HYB 239, containing four mismatched nucleotide bases, were tested to study

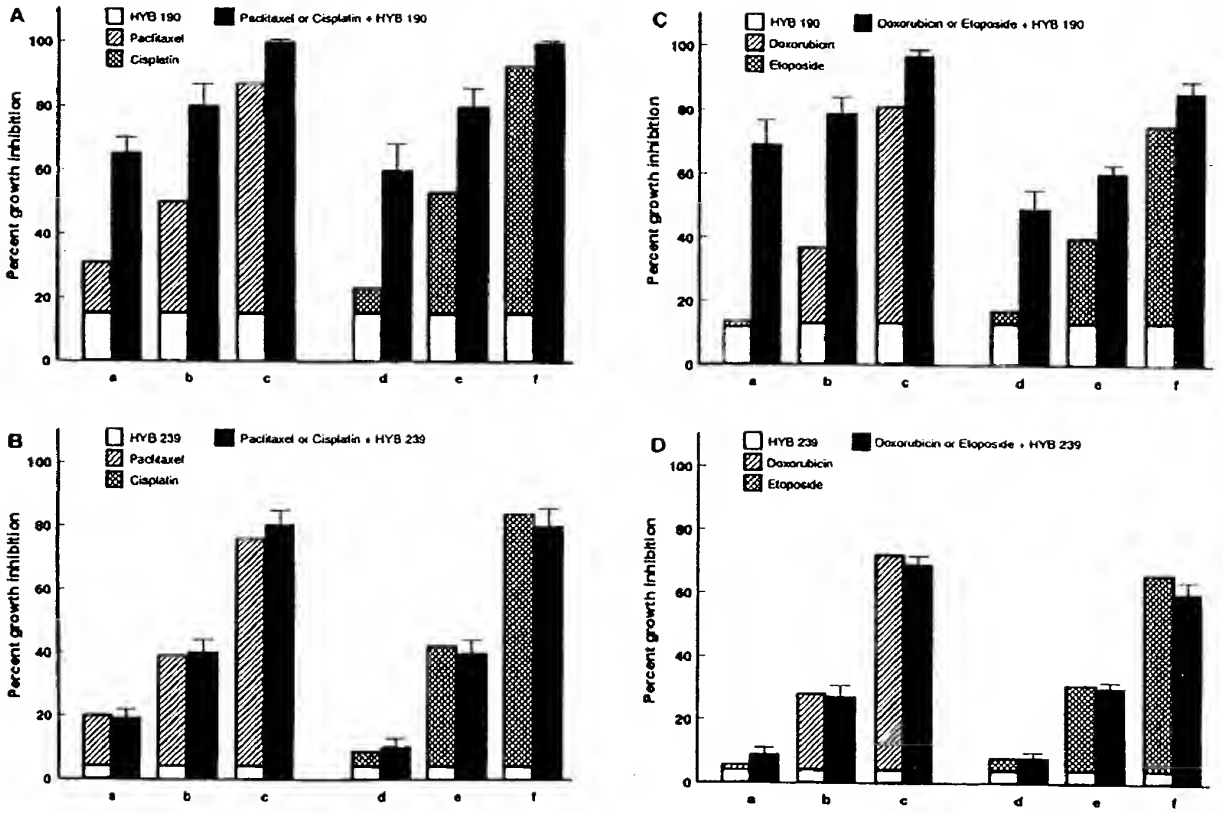

FIG. 2. Effect of different cytotoxic drugs and antisense RIα MBO on the growth of OVCAR-3 cancer cells. (*A*) HYB 190 (0.1 μM) in combination with paclitaxel or cisplatin. (*B*) HYB 239 (1 μM) in combination with paclitaxel or cisplatin. (*C*) HYB 190 (0.1 μM) in combination with doxorubicin or etoposide. (*D*) HYB 239 (1 μM) in combination with doxorubicin or etoposide. The drugs were used at the following doses: a–c, 1, 2.5, and 5 nM paclitaxel; d–f, 5, 10, and 50 ng/ml cisplatin; a–c, 0.01, 0.05, and 0.1 μg/ml doxorubicin; d–f, 0.05, 0.1, and 1 μg/ml etoposide. Data are expressed as percentage growth inhibition in reference to the growth of untreated control cells. The open portion of the bars represents the percentage growth inhibition values for HYB 190 (*A* and *C*) or HYB 239 (*B* and *D*). The striped or squared portion of the bars represents the percentage growth inhibition values for the cytotoxic drugs as indicated in the respective legends. The height of the bars on the left represents the sum of the individual agents' effects and the expected percentage growth inhibition if drugs are additive when used in combination. The total height of the solid bar indicates the actual observed growth inhibition when drugs were used in combination. Therefore, the differences between the heights of the paired bars reflect the magnitude of synergism of growth inhibition. The data represent means and standard errors of triplicate determination of at least two experiments.

their effect on the growth of OVCAR-3, GEO, LS 174T, MDA-MB-231, and MDA-MB-468 human cancer cells in soft agar. Although HYB 190 showed a dose-dependent inhibition of colony formation at doses ranging between 0.01 and 1 μM in all cell lines (Fig. 1*A*), the control MBO HYB 239 at the same doses showed a modest or no growth inhibitory effect (Fig. 1*B*). Western blot analysis after treatment with the antisense RIα MBO in OVCAR-3 ovarian and GEO colon cancer cells confirmed a dose-dependent inhibition of RIα expression in HYB 190- but not in HYB 239-treated cells (data not shown).

Effects of RIα Antisense MBO in Combination with Cytotoxic Drugs. HYB 190 at a dose of 0.1 μM showed an inhibition of OVCAR-3 ovarian cancer cell growth of approximately 15% (Fig. 1*A*), whereas HYB 239 at the same concentration caused less than 10% inhibition (Fig. 1*B*). Therefore, we selected this low dose to study whether any cooperative antiproliferative effect may occur between HYB 190 or HYB 239 and a series of cytotoxic drugs acting by different mechanisms of action in OVCAR-3 cells. When HYB 190 or HYB 239 were added to OVCAR-3 cells treated with different doses of fluorouracil (0.05–0.1 μg/ml), methotrexate (0.05–0.1 μM), vincristine (5–10 ng/ml), or camptothecin (0.05–0.1 ng/ml), which, when used as single agent, showed a growth inhibition between 20% and 60%, an additive growth inhibitory effect was observed on soft agar colony formation (data not shown). A marked synergistic effect was observed when HYB 190 was added to OVCAR-3 treated with paclitaxel, cisplatin, doxorubicin, or etoposide (Fig. 2 *A* and *C*). Conversely, HYB 239 at doses ranging between 0.1 and 1 μM had no such effect when combined with the same cytotoxic agents (Fig. 2 *B* and *D*). The cooperative antiproliferative effect was not restricted to ovarian cancer cells. In fact, when 0.01 μM HYB 190, which caused 22% growth inhibition in GEO colon cancer, or at 0.1 μM, which inhibits 5% of the growth of MDA-MB-231 breast cancer cells, were added to paclitaxel, cisplatin, or doxorubicin, a synergistic growth inhibitory effect was observed. For example, in GEO cells, treatment with 0.01 μM HYB 190 in combination with 1 nM paclitaxel, 0.05 μg/ml cisplatin, or 0.05 μg/ml doxorubicin, which used alone showed 7%, 2%, and 25% growth inhibition, respectively, caused a 60%, 62%, and 78% inhibition of colony formation, respectively.

To study whether this cooperative effect occurs also with other drugs of the same classes, we tested the effect of HYB190 when added to OVCAR-3 cells treated with either the taxane docetaxel or the platinum derivative carboplatin. With each drug, HYB 190 caused a synergistic inhibition of growth. In fact, in cells treated with 0.5 or 1 nM docetaxel, which alone

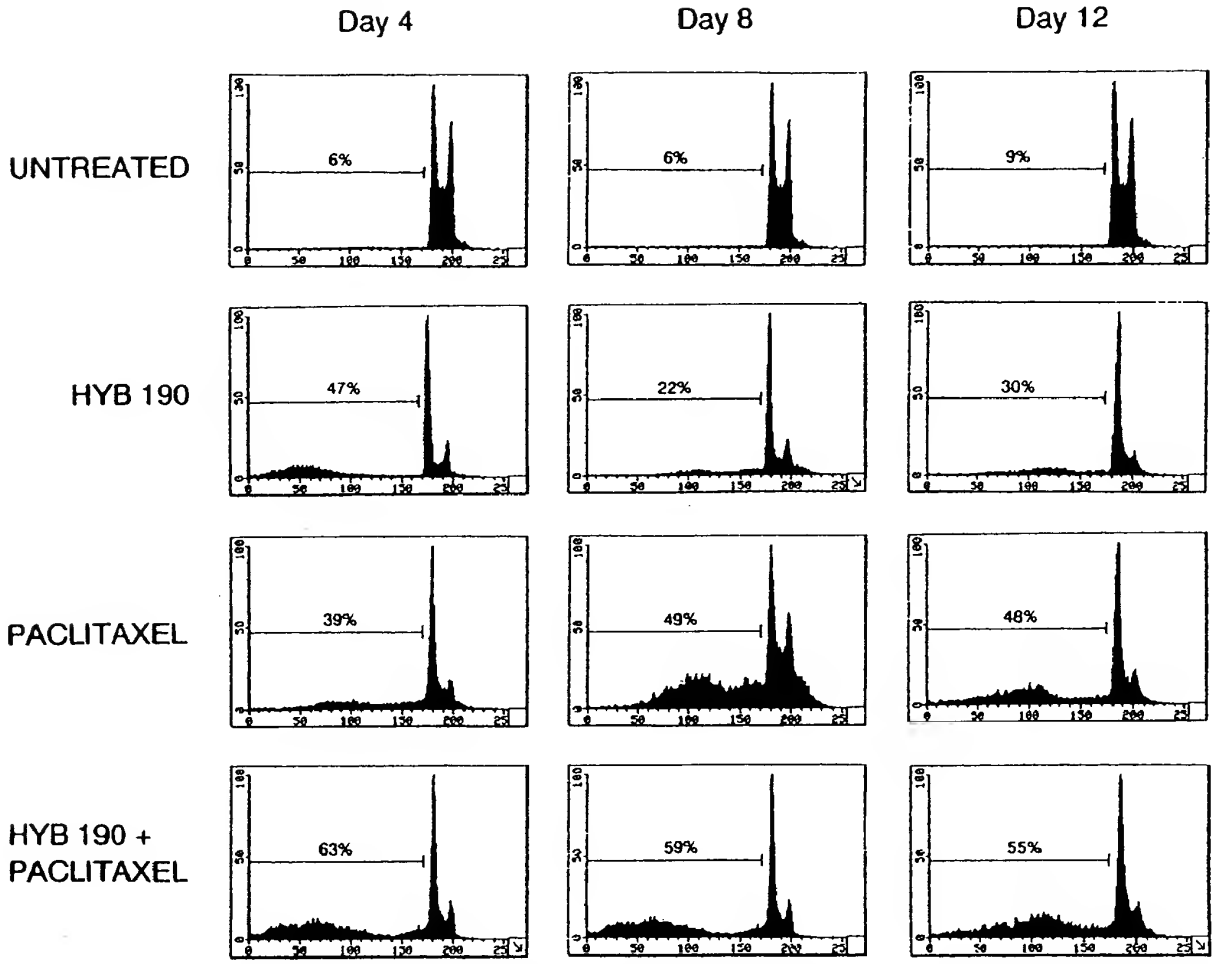

FIG. 3. Flow-cytometric analysis of the effect of 1 nM paclitaxel and/or 0.1 μM HYB 190 on the induction of apoptosis in OVCAR-3 cells. Apoptotic cells are present in the area indicated by a bar on the left side of each histogram. The numbers in each panel represent the percent of apoptotic cells calculated by flowcytometric analysis (25). Data represents one of three different experiments showing similar results.

cause 20% and 45% growth inhibition, respectively, addition of 0.1 μM HYB 190 caused a growth inhibition of 60% and 85%, respectively. An even more dramatic effect was obtained with carboplatin, where the mild growth inhibitory effect produced by this drug at 0.5 μg/ml (6%) or 1 μg/ml (11%) increased to 70% and 90%, respectively, after the addition of 0.1 μM HYB 190 to OVCAR-3 cells.

Cell Cycle Analysis and Evaluation of Apoptosis. We have analyzed the effect of the treatment with the MBOs and/or the cytotoxic drugs on the cell cycle distribution of the cancer cells. After 4 days of treatment with HYB 190, an increase of the cells in G_0/G_1 was observed at all doses between 0.05 and 0.5 μM, whereas 1 nM paclitaxel or 0.05 μM cisplatin alone moderately increased the percent of cells in G_2-M phases. Addition of HYB 190 to the cytotoxic drugs caused accumulation of cells between middle S and G_2-M phases, preventing their progression into M phase. For example, the percent of cells in S and early G_2-M phases was 41% in untreated cells, 32% in cells treated with 0.1 μM HYB 190, 76% in those treated with 1 nM paclitaxel, and 91% in cells treated with both agents. A similar cell cycle distribution was observed at 8 days and 12 days after treatment, except for the fact that the cells treated with the HYB 190 alone began to accumulate in middle S/early G_2-M phases. In the same cell population, we conducted a time-dependent analysis of apoptosis by flow-cytometry (Fig. 3). Although apoptosis was present only in 6–9% of untreated cells, a marked percent of apoptotic cells (46%) was present after 4 days of treatment with 0.1 μM HYB 190 alone and remained over 20% in the cell population examined at 8 and 12 days after treatment. Paclitaxel (1 nM) showed a high percent (about 40% or more) of apoptotic cell death throughout the time course, whereas treatment with both agents in combination always showed, at all time points examined, a percent of apoptosis higher than that obtained with each agent alone.

Effect of RIα Antisense in Nude Mice. To evaluate whether the cooperative effect observed *in vitro* could be obtained also *in vivo*, we used nude mice bearing GEO cell xenografts (27). When large GEO tumors of approximately 0.4 cm^3 were detected, seven mice/group were treated i.p. with paclitaxel (20 mg/kg, the maximum tolerated dose in mice) (26), HYB 190 (10 mg/kg/dose), and HYB 239 (10 mg/kg/dose) used as single agent, or with paclitaxel in combination with either HYB 190 or HYB 239 in a sequential schedule (Fig. 4). As compared with untreated animals, a significant delay of tumor growth was observed in mice either treated with paclitaxel (two-sided $P = 0.05$) or with antisense HYB 190 (two-sided $P = 0.05$), whereas the control oligomer HYB 239 exhibited only a mild growth inhibitory effect. A marked tumor growth inhibition was obtained in mice treated with paclitaxel plus

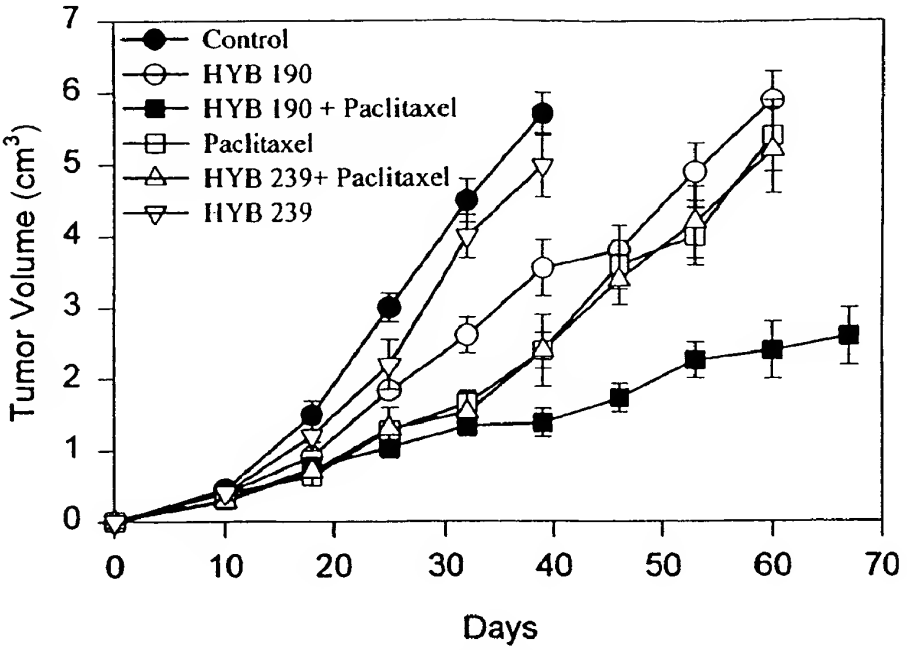

FIG. 4. Effect of the treatment with paclitaxel and/or HYB 190 on the growth of GEO human colon cancer xenografts in nude mice. The administration of each single agent alone or in sequential schedule is described in *Materials and Methods*. Paclitaxel at 400 μg/dose and HYB 190 at 200 μg/dose.

HYB 190, which was statistically significant as compared with control untreated mice (two-sided $P = 0.01$), or mice treated with either paclitaxel (two-sided $P = 0.04$) or HYB 190 (two-sided $P = 0.01$) alone. In contrast, in mice treated with paclitaxel plus the control oligomer HYB 239 the tumor growth inhibition was similar to that determined by the cytotoxic drug alone. Moreover, tumors grew to a size not compatible with normal life in all untreated mice or in those treated with HYB 239 within 40 days after tumor cell injection, and in all mice treated with either paclitaxel, HYB 190 alone, or paclitaxel plus HYB 239 within 60 days. In contrast, all mice treated with the sequential combination of paclitaxel and antisense RIα HYB 190 were still alive and tumor growth was still very slow up to 67 days after GEO cell injection. Finally, no weight loss or other signs of acute or delayed toxicity were observed in this group of mice.

DISCUSSION

Emerging novel strategies of cancer treatment are based on the selective down-regulation of specific targets involved in the process of neoplastic transformation and progression. PKAI seems to be a relevant target for such therapeutic intervention, and antisense oligonucleotides against its RIα subunit have shown promising results in inhibiting cancer cell growth *in vitro* and *in vivo* (13–15). In the present study, we have used a second generation modified oligonucleotide with mixed backbone structure (18, 24) designed to target PKAI. Such MBOs have shown better pharmacokinetic and toxicology profile *in vivo* (24). The 18-mer RIα antisense MBO HYB 190 showed a dose-dependent inhibitory effect on different human cancer cell types, including ovary, colon, and breast, at submicromolar concentrations ranging between 0.01 and 1 μM. The effect appeared to be sequence-specific, as HYB 239, a similar MBO with only four mismatched nucleotide bases, at the same concentrations was ineffective in inhibiting cancer cell growth. The HYB 190 is complementary to the same sequence of RIα targeted by an antisense oligonucleotide previously shown effective in inhibiting PKAI expression and function (15). Indeed, HYB 190, but not HYB 239, inhibited the expression of RIα protein in OVCAR-3 and GEO colon cells. To evaluate whether any cooperative effect may exist between cytotoxic drugs and a novel PKAI selective down-regulator such as the HYB 190 MBO, we tested the effect of HYB 190 or its control sequence HYB 239 in combination with cytotoxic drugs of different classes in several cancer cell lines. We have demonstrated that HYB 190 is additive when added to cells treated with the antimetabolites fluorouracil or methotrexate, the vinca alcaloid vincristine, or the topoisomerase I-selective drug camptothecin. A marked synergistic effect was observed when HYB 190 was used in combination with the taxanes paclitaxel and docetaxel, the platinum derivatives cisplatin and carboplatin, and the topoisomerase II-selective agents doxorubicin and etoposide. In contrast, no cooperative effect was obtained when the same drugs were added to the same or higher doses of control MBO HYB 239. It is likely that the inhibition of the PKAI-related mitogenic pathway plays a key role in the observed cooperative effect with the cytotoxic drugs. In fact, we have recently shown that 8-Cl-cAMP, another selective inhibitor of PKAI expression, has a synergistic growth inhibitory effect with taxanes and platinum-derived compounds in a variety of cancer cell types (29, 30).

In the attempt to understand the kinetics of these events, we analyzed the effect on cell cycle and apoptosis of the antisense compounds with or without the cytotoxic drugs. Whereas paclitaxel causes accumulation of cells in G_2-M phases, the antisense HYB 190 tends to first accumulate cells in G_0/G_1 and, later, in S/G_2-M phase. These results are consistent with our previous report that PKAI is important in the G_1-S transition (3) and with our most recent observation that PKAI, together with the surge at the G_1-S transition, has a second peak of expression at the late S/early G_2 phase (31). Along with these cell cycle perturbations, apoptosis seems to be present very early after treatment with either RIα antisense or the cytotoxic drug alone. When the antisense MBO is administered in combination with the cytotoxic drug in the sequen-

tial treatment, a marked increase in the S-G_2 phase is observed throughout the course of the experiment. Interestingly, a consistent amount of apoptotic cells, over 50%, is present for several days after treatment, suggesting that cells undergo several rounds of apoptosis. These data seem in agreement with a recent study suggesting that uncoupling between increase of S phase and inhibition of cell division is a major event occurring after treatment with certain cytotoxic drugs inducing apoptosis (32).

We next evaluated whether the cooperative effect obtained *in vitro* could also be reproduced *in vivo* in nude mice bearing GEO human colon cancer xenografts. We have shown that, unlike the control oligo HYB 239, which only mildly inhibited GEO tumor growth, HYB 190 significantly delayed tumor growth as compared with control mice. Moreover, whereas HYB 239 combined with paclitaxel had an effect similar to that of paclitaxel alone, combination of paclitaxel with HYB 190 determined a significantly increased tumor growth inhibition as compared with untreated mice or to mice treated with each single agent. In addition, all control mice or mice treated with HYB 239 died within 40 days whereas mice treated with HYB 190 alone, paclitaxel alone, or paclitaxel in combination with HYB 239 died within 60 days. In contrast, at the same time point, all animals treated with paclitaxel and HYB 190 (*i*) showed over 50% tumor growth inhibition as compared with mice treated with either agent alone, (*ii*) were alive at 67 days, and (*iii*) the tumor growth was still very slow although the combination treatment was completed 15 days after tumor cell injection. Remarkably, HYB 190 significantly increased the activity of paclitaxel but not the toxicity, considering that the taxane was used at the maximum tolerated dose in nude mice (26).

Our study reports that a relevant cooperative effect toward tumor growth inhibition can be achieved *in vitro* and *in vivo* by combining specific cytotoxic drugs with second generation oligodeoxynucleotides targeting PKAI. Moreover, we have provided evidence that the inhibitory effect correlates with a marked induction of apoptosis and does not result in increased toxicity. Experiments are ongoing to study whether the synergistic inhibitory effect correlate not only with suppression of RIα, but also with that of other relevant growth regulators such as growth factors and angiogenic factors. Taken together, these data suggest that selective down-regulation of PKAI, a key mitogenic signal transducer, is an important event able to markedly increase the antitumor efficacy of certain conventional cytotoxic drugs. As HYB 190 is a prototype of novel second generation oligodeoxynucleotides (the MBOs), which have shown an improved *in vivo* pharmacologic profile without toxicity (24), our study provides a rationale for translating this combination treatment strategy into a clinical setting.

This study was supported by the Associazione ttaliana per la Ricerca sul Cancro and from the Progetto Finalizzato-Applicazioni Cliniche della Ricerca Oncologica (Consiglio Nazionale delle Ricerche).

1. Cho-Chung, Y. S. & Clair, T. (1993) *Pharmacol. Ther.* **60**, 265–288.
2. Taylor, S. S., Buechler, J. A. & Yonemoto, W. (1990) *Annu. Rev. Biochem.* **59**, 971–1005.
3. Tortora, G., Pepe, S., Bianco, C., Baldassarre, G., Budillon, A., Clair, T., Cho-Chung, Y. S., Bianco, A. R. & Ciardiello, F. (1994) *Oncogene* **9**, 3233–3240.
4. Ciardiello, F., Pepe, S., Bianco, C., Baldassarre, G., Ruggiero, A., Bianco, C., Selvam, M. P., Bianco, A. R. & Tortora, G. (1993) *Int. J. Cancer* **53**, 438–443.
5. Ciardiello, F., Tortora, G., Kim, N., Clair, T., Ally, S., Salomon, D. S. & Cho-Chung, Y. S. (1990) *J. Biol. Chem.* **265**, 1016–1020.
6. Tortora, G., Damiano, V., Bianco, C., Baldassarre, G., Bianco, A. R., Lanfrancone, L., Pelicci, P. G. & Ciardiello, F. (1997) *Oncogene* **14**, 923–928.
7. Simpson, J. B. B., Ramage, A. D., Hulme, M. J., Burns, D. J., Katsaros, D., Langdon, S. & Miller W. R. (1996) *Clin. Cancer Res.* **2**, 201–206.
8. Miller, W. R., Watson, D. M. A., Jack, W., Chetty, U. & Elton, R. A. (1993) *Breast Cancer Res. Treat.* **26**, 89–94.
9. Rohlff, C., Clair, T. & Cho-Chung, Y. S. (1993) *J. Biol. Chem.* **268**, 5774–578.
10. Tortora, G., Clair, T. & Cho-Chung, Y. S. (1990) *Proc. Natl. Acad. Sci. USA* **87**, 705–708.
11. Ally, S., Clair, T., Katsaros, D., Tortora, G., Yokozaki, H., Finch, R. A., Avery, T. L. & Cho-Chung, Y. S. (1989) *Cancer Res.* **49**, 5650–5655.
12. Ramage, A. D., Langdon, S. P., Ritchie, A. A., Burns, D. J. & Miller, W. R. (1995) *Eur. J. Cancer* **31A**, 969–973.
13. Tortora, G., Yokozaki, H., Pepe, S., Clair, T. & Cho-Chung, Y. S. (1991) *Proc. Natl. Acad. Sci. USA* **88**, 2011–2015.
14. Yokozaki, H., Budillon, A., Tortora, G., Meissner, S., Beaucage, S. L., Miki, K. & Cho-Chung, Y. S. (1993) *Cancer Res.* **53**, 868–872.
15. Nesterova, M. & Cho Chung, Y. S. (1995) *Nat. Med.* **1**, 528–533.
16. Ratajczak, M. Z., Kant, J. A., Luger, S. M., Hijiya, N., Zhang, J., Zon, G. & Gewirtz, A. M. (1992) *Proc. Natl. Acad. Sci. USA* **88**, 11823–11827.
17. Ma, L. & Calvo, F. (1996) *Fundam. Clin. Pharmacol.* **10**, 97–115.
18. Agrawal, S. (1996) *Trends Biotechnol.* **14**, 376–387.
19. Monia, B. P., Johnston, J. F., Geiger, T., Muller, M. & Fabbro, D. (1996) *Nat. Med.* **2**, 668–692.
20. Leonetti, C., D'Agnano, I., Lozupone, F., Valentini, A., Geiser, T., Zon, G., Calabretta, B., Citro, G. & Zupi G. (1996) *J. Natl. Cancer Inst.* **88**, 419–429.
21. Skorski, T., Nieborowska-Skorska, M., Wlodarski, P., Perrotti, D., Hoser, G., Kawiak, J., Majewski, L., Christensen, L., Iozzo, R. V. & Calabretta, B. (1997) *J. Natl. Cancer Inst.* **89**, 124–133.
22. Agrawal, S., Temsamani, J. & Tang, J. Y. (1991) *Proc. Natl. Acad. Sci. USA* **88**, 7595–7599.
23. Akhtar, S. & Agrawal, S. (1997) *Trends Pharmacol. Sci.* **18**, 12–18.
24. Agrawal, S., Jiang, Z., Zhao, Q., Shaw, D., Cai, Q., Roskey, A., Channavajiala, L., Saxinger, C. & Zhang, R. (1997) *Proc. Natl. Acad. Sci. USA* **94**, 2620–2625.
25. Nicoletti, I., Migliorati, G., Pagliacci, M. C., Grignani, F. & Riccardi, C. (1991) *J. Immunol. Methods* **139**, 271–279.
26. Fan, Z., Baselga, J., Masui, H. & Mendelsohn, J. (1992) *Cancer Res.* **53**, 4637–4642.
27. Ciardiello, F., Damiano, V., Bianco, R., Bianco, C., Fontanini, G., De Laurentiis, M., De Placido, S., Mendelsohn, J., Bianco, A. R. & Tortora, G. (1996) *J. Natl. Cancer Inst.* **88**, 1770–1776.
28. Fleiss, J. L. (1981) *Statistical Methods for Rates and Proportions* (Wiley, New York), 2nd Ed.
29. di Isernia, G., Ciardiello, F., Sandomenico, C., Pepe, S., Bianco, A. R. & Tortora, G. (1996) *Int. J. Oncol.* **9**, 1233–1237.
30. Tortora, G., di Isernia, G., Sandomenico, C., Bianco, R., Pomatico, G., Pepe, S., Bianco, A. R., and Ciardiello, F. (1997) *Cancer Res.*, in press.
31. Cho-Chung, Y. S., Nesterova, M., Kondrashin, A., Noguchi, K., Srivastava, R. & Pepe, S. (1997) *Antisense Nucleic Acid Drug Dev.*, **7**, 217–223.
32. Waldman, T., Lengauer, C. Kinzler, K. W. & Vogelstein, B. (1996) *Nature (London)* **381**, 713–716.

APPENDIX B

Selecting effective antisense reagents on combinatorial oligonucleotide arrays

Natalie Milner, Kalim U. Mir, and Edwin M. Southern*

*Department of Biochemistry, University of Oxford, South Parks Road, Oxford OX1 3QU, UK. *Corresponding author (e-mail: ems@bioch.ox.ac.uk).*

Received 14 February 1997; accepted 24 April 1997

An array of 1,938 oligodeoxynucleotides (ONs) ranging in length from monomers to 17-mers was fabricated on the surface of a glass plate and used to measure the potential of oligonucleotide for heteroduplex formation with rabbit ß-globin mRNA. The oligonucleotides were complementary to the first 122 bases of mRNA comprising the 5' UTR and bases 1 to 69 of the first exon. Surprisingly few oligonucleotides gave significant heteroduplex yield. Antisense activity, measured in a RNase H assay and by in vitro translation, correlated well with yield of heteroduplex on the array. These results help to explain the variable success that is commonly experienced in the choice of antisense oligonucleotides. For the optimal ON, the concentration required to inhibit translation by 50% was found to be five times less than for any other ON. We find no obvious features in the mRNA sequence or the predicted secondary structure that can explain the variation in heteroduplex yield. However, the arrays provide a simple empirical method of selecting effective antisense oligonucleotides for any RNA target of known sequence.

Keywords: antisense, oligonucleotide, optimization, arrays, secondary structure

Antisense technology holds potential for therapy and for the study of gene function. It also offers an alternative to "knockout" techniques in the characterization of the large number of sequences emerging from genome projects. The concept is appealing: The reagents are readily synthesized, and can be used to down-regulate the expression of any mRNA of known sequence. Oligonucleotides (ONs) targeted to sequences only a few bases apart on the mRNA can give rise to quite different antisense effects. The interaction between target and antisense agent is determined in part by their secondary and tertiary structures, which are difficult to predict[1]. Existing methods for energy calculations do not predict the results that are observed and so there has been a move towards a more empirical approach to antisense site selection. Stull et al. recently reported a study of 37 ONs targeted against murine tumour necrosis factor-α[2]. Each oligonucleotide was individually synthesised and evaluated using a gel-shift binding assay. In another case 100 different 20-mers were synthesized, targeting various genes of HSV-1[3].

We demonstrate a combinatorial technique that allows simultaneous assessment of all possible ONs within a given region identifying sequences open to duplex formation. An oligonucleotide "scanning" array reduces the number of synthesis steps while providing a parallel and exhaustive analysis of all ONs in the region to be targeted. We chose the well-studied example of rabbit β-globin as the target mRNA and synthesised an array of antisense oligodeoxynucleotides against 122 bases at the 5' end. An in vitro transcript was hybridized to the array which comprised all ONs up to a length of 17 bases.

We found that intramolecular base pairing sequesters much of the sequence, preventing the intermolecular pairing essential to antisense activity. However, those ONs which give high duplex yield on the array proved to be effective antisense agents in in vitro RNase H and translation studies.

Results

Hybridization to the scanning array. Under conditions close to equilibrium, hybrid yield for the β-globin mRNA was very low across most of the array (Fig. 1A). There was no detectable hybridization to bases 1 to 37 or 76 to 90 of the mRNA, almost half of the region scanned by the array. Only one sequence gave high duplex yield, a 15-base ON complementary to bases C46–C60. This sequence is also contained within two 16-mer and three 17-mer ONs (Fig. 1B). The yield of these six heteroduplexes was at least three times that of any other ON and five times that of the 17-mer selected by Cazenave et al.[4], located five bases downstream. An area of weak hybridization starts at base C38. These hybrids include bases C40–A44 which are predicted to be unpaired in the RNA (Fig. 2). Two other regions gave weak but detectable hybridization: 14 ONs hybridized to a region starting at base A61 and ending at C91; a second region of weak hybridization starts at base C94. This region contains a run of eight purines, interrupted by a cytosine, with four consecutive guanines which may help to stabilise the heteroduplex.

In a region of 122 bases around the start codon of the β-globin mRNA over 60% of the 106 complementary 17-mer ONs gave duplex yields less than one tenth that of the optimal ON. Sixty-two percent had an intensity less than one tenth that of the highest and all but five had a heteroduplex yield of less than 40% of the highest yield. The top three are derived from the core 15-base optimal ON and the fourth is one base shifted starting at base A48 (Fig. 1B). The fifth ON (in the 40% to 50% range) is the 17-mer starting at base C94: the beginning of an area of moderate hybridization.

In contrast to the result with RNA, single-stranded DNA of the same base sequence and length, which has weaker intramolecular bonding than RNA, hybridized with moderate yield to most of the array (data not shown). This result verified the integrity of the array synthesis.

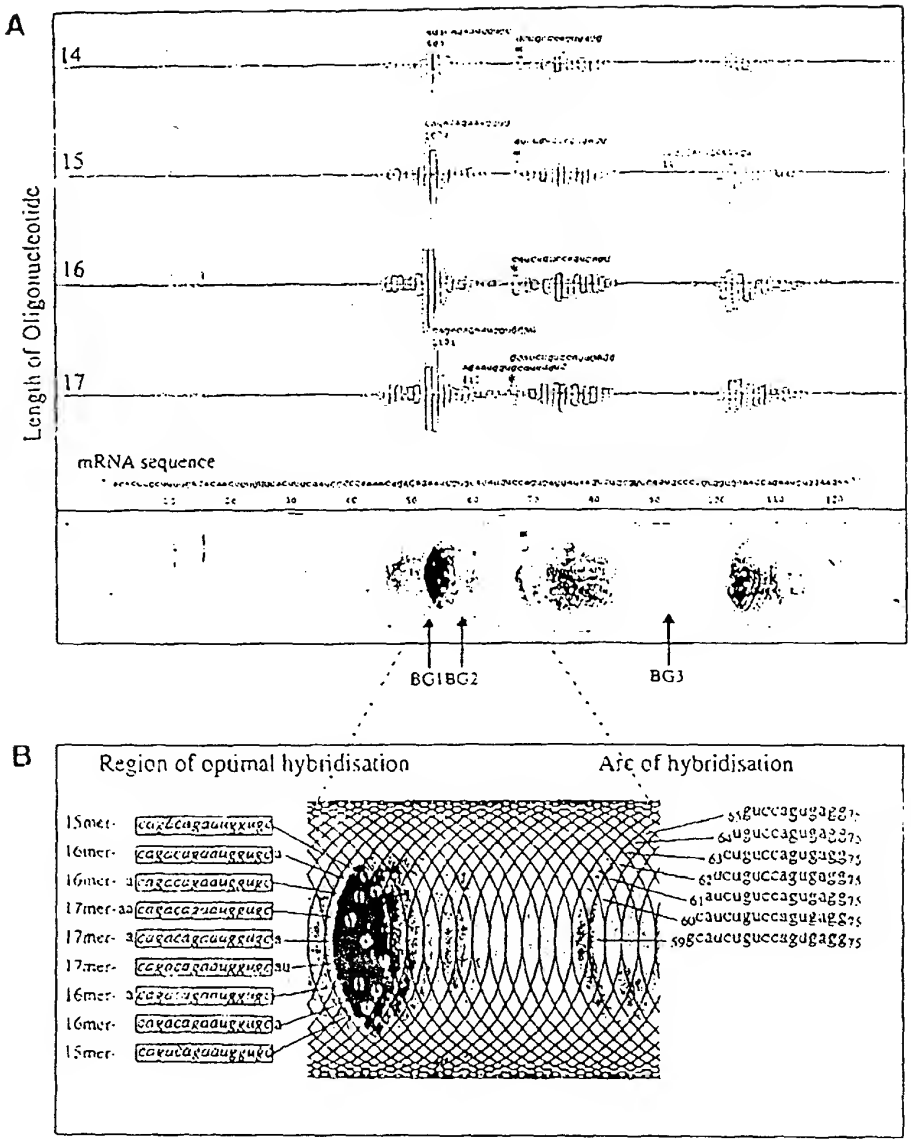

Figure 1. (A) Hybridization of ^{32}P-labeled ß-globin transcript to an array of ONs (monomers to 17-mers) complementary to bases 1–122. The two halves of the array are integrated separately and are shown by bars above and below the center line. Each histogram represents a set of ONs of one length (shown on the left). The positions, sequences and integrated intensity values of the oligonucleotides BG1, BG2, and BG3, used in antisense experiments are indicated. The asterisks mark an arc shaped region of hybridization (see below). The sequences as written represent the mRNA sequence, the complements of the antisense ON sequences. (B) The area of the array around the optimal ON. The core 15-mer sequence is boxed and written in italics. The position and sequence of each ON is indicated. BG1 is the right most 17-mer comprising the 15-mer with an additional "au" at the right hand end. Also shown is the position of the "arc" of oligonucleotides, each of which gives the same yield of heteroduplex and each of which terminates in the same base at the 5′ end.

Antisense activity of oligonucleotides with different binding strengths. Three ONs, with different heteroduplex yields, were chosen for study by in vitro translation and RNase H assay. BG1 was complementary to bases C46–U62 and includes the high yielding 15-mer; a length of 17 bases was chosen for a more direct comparison with Cazenave's ON. BG2 (A51–C67) was the antisense oligonucleotide studied by Cazenave et al. BG3 (C85–U99, gave no detectable hybridization (Fig. 1A).

RNase H mediated cleavage. To compare the effectiveness of BG1 and BG2 at recruiting RNase H, the oligonucleotides were added to labeled β-globin transcript over a range of concentrations (Fig. 3A). At equimolar ratio of ON to mRNA, BG1 caused cleavage of 50% of the transcript as compared to only 9% for BG2. In the higher concentration ranges, similar effects were obtained with tenfold lower concentration of BG1 as compared with BG2. These results indicate that BG1 is five to ten times more effective than BG2.

The rate of reaction could be limited by hybrid formation or by RNase H activity. BG1 and BG2 were added to β-globin transcript at a 100:1 molar excess and sampled over time (Fig. 3B). For BG1 all of the transcript was cleaved by 1 min. For BG2, the reaction

Table 1. The concentrations of ON required to produce 50% inhibition of rabbit ß-globin protein product.

Position and designation	Hybrid yield	Oligo concentration	Ratio concentration oligo:ß-globin	% Inhib. in WGE
47–62 BG1	980	0.1 µM	4:1	50%
51–67 BG2	192	0.5 µM	20:1	50%
85–99 BG3	8	1 µM	40:1	0%
3–19	28	0.2 µM	50:1	50%'
44–54	16	3 µM	750:1	50%"

Concentrations are final concentrations in the translation reaction. The final concentration of β-globin mRNA was 24 nM. In the results taken from references 6 and 16 the concentration was 4 nM.

rate was much slower—at 1 min only 42% of the transcript had been cleaved. The rate difference shows that the reaction rate was limited by heteroduplex formation. Prehybridization of the ON increased the amount of cleavage product over that seen when the ON was added with the enzyme, confirming the dependence of the rate on the hybridization reaction (data not shown).

In vitro translation. Correlation between extent of hybridization and efficacy as antisense reagents extended to in vitro translation in wheat germ extract (WGE) (Fig. 4). At high concentrations (10 μM), each oligonucleotide caused nonspecific inhibition of both α- and β-globin synthesis. However, at 1 μM inhibition was specific: BG1 completely blocked β-globin; BG2 reduced it to 36% and neither affected α-globin translation; BG3 had no effect on either β- or α-globin. Further reduction in concentration showed that for BG1 the minimum concentration needed to give complete, specific inhibition of translation was between 0.1 and 0.2 μM as compared to 1–10 μM for BG2 (data not shown).

Table 1 summarizes the comparison of in vitro translation studies in WGE of ONs targeted to the 5′ end of rabbit β-globin. BG1 requires a concentration five times lower than any other ON to effect 50% inhibition of translation.

Discussion

The regulatory cap region is often chosen as an antisense target site. Specifically for β-globin, it is thought to be relatively open and accessible to facilitate high levels of translation[3]. However, we found insignificant level of hybridization to the first 37 bases at the 5′ end of the mRNA. Other work (in systems where RNase H is present) has shown that ONs targeted to the cap region of this gene are relatively poor antisense agents[4,5].

The sequence and predicted secondary structure of the mRNA give few clues as to what makes BG1 particularly amenable to duplex formation (Fig. 2). A run of seven ribopurines interrupted by a cytosine, aagacaga, may stabilize the duplex but six bases of this sequence are paired in a relatively stable stem in the predicted RNA structure. Runs of ribopurines are known to stabilize DNA:RNA heteroduplexes[3], but alone are not sufficient to induce heteroduplex formation as bases G72–G80, gaggagaag, four of which are predicted to be unpaired, are present in hybrids which gave only modest yields.

Duplex yield is not necessarily increased by increasing the length of the oligonucleotide; BG1 is a clear example where the 15-mer gives the same yield as cognate 17-mers (Fig. 1B). We have found for other RNAs that short oligonucleotides give higher yield than longer ones. We speculate that the longer oligonucleotides have internal base pairing which prevents heteroduplex formation, or that duplex formation is inhibited by dangling ends of oligonucleotide which cannot fit into the folded structure of the RNA.

It seems likely that duplex formation is confined to those regions in the RNA which provide an accessible substructure. This substructure will include a site for nucleation, which must have unpaired bases. Duplex formation will progress from the nucleation site through a 'zippering' process, and stop when this process meets an energy barrier. Such barriers may include the ends of stems or sharp turns in the folded RNA. The yield of heteroduplex

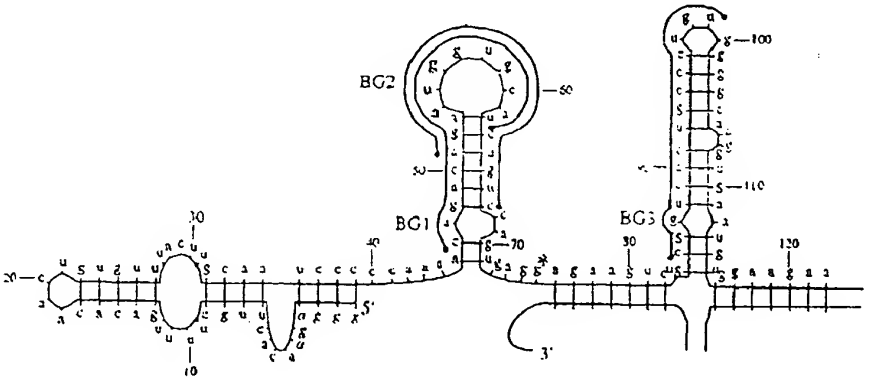

Figure 2. Prediction of the secondary structure of rabbit ß-globin mRNA[6]. The region shown is that covered by the scanning array. The 17 RNA polymerase consensus sequence (shown in italics) produces a very small local structural change which should not affect hybridization. The positions of the oligonucleotides used in antisense experiments are indicated. The critical base, G75, in the "arc" pattern of hybridization is marked by an asterisk.

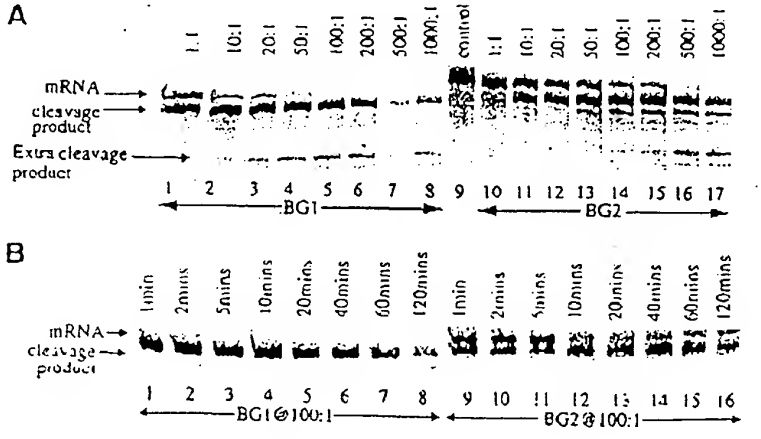

Figure 3. (A) Effect of antisense ON concentration on in vitro RNase H activity against rabbit ß-globin mRNA. The full length mRNA of 608 bases and the cleavage product of about 550 bases are indicated. (B) A time-course of in vitro RNase H activity with BG1 and BG2 at 1 μM (a 100:1 molar excess) and transcript at 10 nM. The extra cleavage product is due to a six-base region of complementarity (bases 431–436 of the mRNA) to BG1 and BG2.

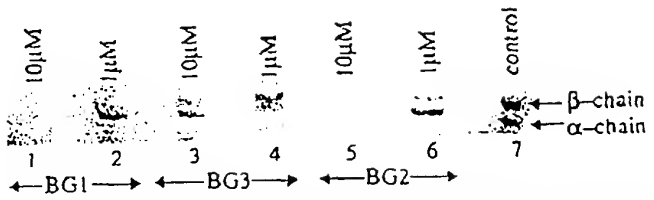

Figure 4. In vitro translation of rabbit α- and β-globin mRNA in the presence of antisense oligos BG1, BG2, and BG3. The upper band is the β-globin protein product and the lower the α-globin protein. The products were analysed by TAU-PAGE[11].

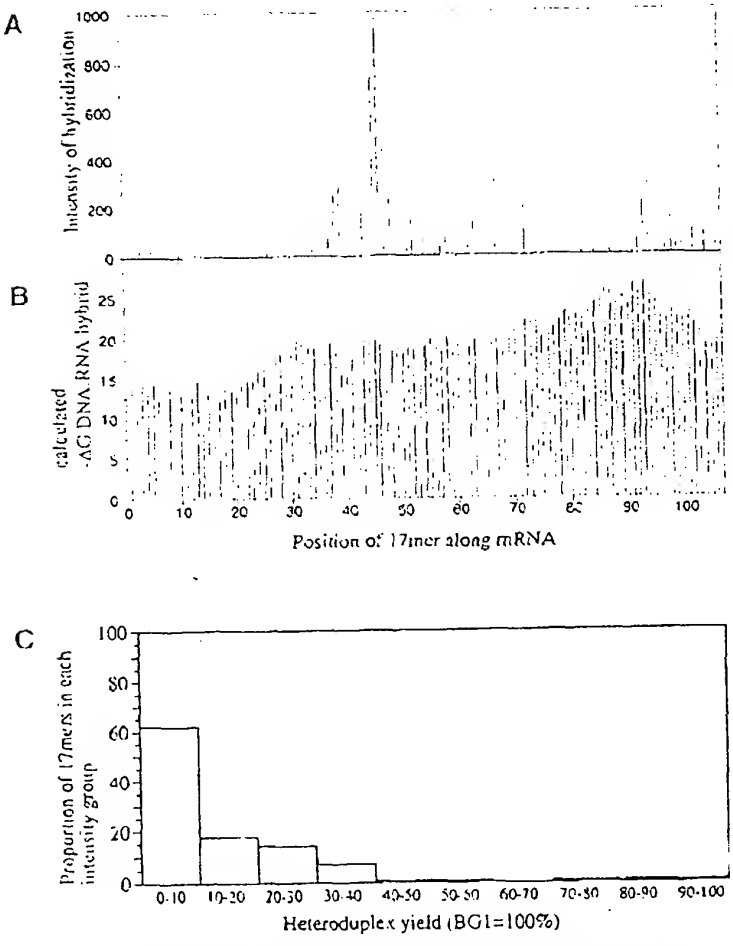

Figure 5. (A) Integrated signal intensities of the 17-mer heteroduplexes across the array, taken from Figure 1A. The first bar corresponds to the heteroduplex yield between the mRNA and the DNA complement of bases A1–C17. The histogram moves sequentially along the mRNA demonstrating the large range in heteroduplex yield. (B) The calculated negative free energies of formation of the 17-mer heteroduplexes. (C) Distribution of heteroduplex yield of the 106 17-mers. The values of the signal intensities were those shown in Figure 1A.

will be determined by the association and dissociation rates: The association rate is determined by the formation of a nucleation complex and subsequent zippering; the dissociation rate is determined by the stability of the formed hybrid. Both of these are affected by structural features in the RNA.

The arc pattern of hybridization reveals an interesting structural element in the RNA (Fig. 1B). The group of ONs in this arc all share the same 5′ end, G75, and reduce in length from the 3′ end. In the structure prediction (Fig. 2) G75 is a free, unpaired base at the end of a stem. With this base at its 5′ end, the ON is apparently able to form a stable duplex by unwinding the two stems upstream of it, U62–C67 and G70–U71. Adding a base to the 5′ end or removing the complement of G75 reduces heteroduplex yield dramatically. G75 may provide a stable nucleation point that is particularly well configured for hybridization to the free 5′ end of the oligonucleotide. Once formed the hybrid may gain added stability by stacking onto the adjacent stem A76–C82.

It is likely that the oligonucleotides tethered at their 3′ ends would nucleate from the free 5′ end, and behave differently from ONs in solution. Although this is a concern, our results gave good correlation between hybrid yield on the array and RNase H activity. In another study, heteroduplex yield on the array correlated well with in vivo and in vitro cell culture antisense activities. Monia et al.[9] tested 34 phosphorothioate ONs mostly in the 5′ and 3′ UTRs for specific inhibition of C-*raf*-1 kinase gene expression, and found one, ISIS 5132, to be an order of magnitude more effective than any other at reducing gene expression in a cell culture assay. ISIS 5132 was also shown to suppress the growth of tumors engrafted in nude mice. In a blind experiment, analysis on a scanning array picked out ISIS 5132 as one of the two high-yielding ONs in 100 base region around ISIS 5132 (data not shown). For the rest of the ONs covered by the array, heteroduplex yield closely followed the antisense activity.

Our results confirm that the susceptibility of a target RNA to antisense interaction varies greatly from one part of the sequence to another and indicate that it is determined by the potential to form heteroduplex. Few sites in the target are open to interaction in the 5′ end of the β-globin mRNA. This is typical of analyses we have done on several mRNAs and in all parts of the sequence (data not shown). At each of the accessible sites very few ONs, often only one, are able to form duplex. These results were not predicted by calculations based on the free energy difference between the reactants—the folded mRNA and the single-stranded ON—and the heteroduplex product. Our calculations were improved over the earlier calculations of Stull et al.[10] as we were able to incorporate recently derived free energy values for RNA:DNA duplexes[11]. The plot for β-globin shows no apparent correlation between the estimated ΔG of heteroduplex formation (Fig. 5B) and the extent of hybrid formed on the array (Fig 5A).

Libraries of random or semi-random ONs have been used to map sites accessible to RNase H along the target mRNA[12,13]. This method reveals open areas, but to pinpoint precise locations Lima et al. individually synthesized many overlapping and different length ONs around the RNase H accessible sites. We envisage a strategy which uses RNase H to scan the whole RNA molecule to locate open regions which can then be examined in detail on oligonucleotide arrays. Wagner et al. recently demonstrated that an

octanucleotide was enough to give specific antisense activity. The exact location was important, suggesting the major determinant to be the RNA structure at the binding site[1]. Taken with our studies these observations make clear the difficulty of finding good candidates for antisense sequences by methods which are not based on experimental measurements.

The method used in this study can be adapted to any analogue for which there is appropriate solid phase chemistry, it has been used to make arrays of phosphorothioate,2'-O-methyl and other derivatives. With other modifications, it could be used for synthesis of peptide nucleic acid analogues (PNAs). It is clear that selecting oligonucleotides which interact well with the target has important consequences for their efficacy as antisense agents. For therapeutic agents this translates into enhanced specificity and a reduction in dose, with attendant reductions in cost and toxicity.

Experimental protocol

Array fabrication. The array was made as described[11]. Briefly, a glass plate (600 mm × 350 mm) was derivatized with a covalently attached hexaethylene glycol linker[14]. Oligonucleotide synthesis was performed directly onto the coated glass using a circular reaction chamber. The diameter of the chamber was 42.5 mm and the offset between base couplings was 2.5 mm, creating oligonucleotides up to a maximum length of seventeen bases. Oligonucleotide synthesis used standard reagents for phosphoramidite chemistry, omitting the capping step. Synthesis was on an adapted Applied Biosystems (Foster City, CA) 381A synthesizer. Deprotection of the array in 30% ammonia solution was carried out as described[15] in a specially constructed nylon chamber.

Hybridization to the array. Hybridization solution (in vitro synthesized and ^{32}P UTP radiolabeled transcript (50 fmol), NaCl (1 M), TE (10 mM, pH 8.0), SDS (0.01%) in a 500 µl volume) was applied evenly along the length of a glass backing plate. The plate carrying the scanning array was placed face down on top of the backing plate ensuring no air bubbles were trapped. The hybridization assembly was placed in a sealed moist chamber, and left to hybridize for 15 h at 30°C. The array was washed briefly in hybridization solution at 30°C, blotted dry and exposed to a storage phosphor screen (Fuji ST111, Tokyo, Japan) for 20 h. The screen was scanned in a Molecular Dynamics (Sunnyvale, CA) 400A PhosphorImager. The analysis and quantitation of the image used xvseq (data not shown). To analyze the resulting image a template comprising a series of overlapping circles is placed over the image (Fig. 1B) and each region within areas defined by the template is integrated. The integrated values represent the intensity of hybridization of each ON and are displayed as histograms. The quantitation was performed using xvseq. The array is symmetrical about the horizontal axis, providing a duplicate measurement for each ON. The array was stripped of hybridized target by soaking in TE/SDS at 55°C to 65°C, ready for reuse.

Oligonucleotide preparation. Oligodeoxyribonucleotides were synthesised using an Applied Biosystems 381A synthesizer with trityl on and purified using ABI oligonucleotide purification columns (OPC). Purity was evaluated by analysis on a 20% denaturing polyacrylamide gel (1xTBE, 1500V, 30mA, 1.5 h) after 5' terminal labelling with T4 polynucleotide kinase and γ^{32}P-ATP. The sequences of oligonucleotides used were: BG1 5'-atgcaccatttctgtctg-3' BG2 5'-gacagatgcaccatttct-3'BG3 5'-acagggcagtgaccg-3'.

Preparation of labeled RNA transcript. A double stranded DNA template carrying the T7 transcription promoter sequence was generated using the RT-PCR protocol of Maniatis et al.[17] using purified rabbit globin mRNA (Gibco BRL, Paisley, UK). The PCR product was purified using a Pharmacia (Uppsala, Sweden) Microspin column, and transcribed using the standard transcription protocol incorporating 20 µCi α ^{32}P-UTP (1000–3000 Ci/mmol). The product was purified by G25 Sephadex column chromatography. The molecular weight of the transcript was evaluated prior to hybridization by electrophoresis on a 6% denaturing polyacrylamide gel (1xTBE, 1500 V, 30 mA, 1.5 h).

Ribonuclease H reactions. Reactions were according to manufacturer's instructions using 10 nM labeled in vitro transcript and various concentrations of oligonucleotides. The reagents were incubated at 30°C and the reaction was started by addition of the oligonucleotide. Reactions were for 2 h and stopped by the addition of formamide (30%), EDTA (0.2 M). For time-course assays, a 40 µl reaction volume was used. The products were analyzed on a 6% denaturing polyacrylamide gel. Quantitation used Molecular Dynamics ImageQuant software.

In vitro translation. Rabbit globin mRNA (0.3 µg) was added to a translation mixture containing wheat germ extract, amino acids (80 µM each), potassium acetate (100 mM) and oligonucleotides at various concentrations. The reaction was started by the addition of 15 µCi ^{35}S methionine (1000 Ci/mmol) and incubated for 2 h at 25°C. The final concentration of β-globin mRNA in the reaction was 24 nM. Products were analysed by gel electrophoresis on a 12% acrylamide gel containing 0.7% Triton-X100 and 6 M urea, in 5% acetic acid buffer using the method described by Rovera et al.[18]

Acknowledgments

We wish to thank J.K. Elder for his assistance with the computational work, H. Salter for the thermodynamic data, S.C. Case-Green for supplying the derivatized glass plate and M. Johnson for design of the array synthesizer. The work was supported by a HGMP-MRC grant.

1. Lima, W.F., Monia, B.P., Ecker, D.J., and Freier, S.M. 1992. Implication of RNA structure on antisense oligonucleotide hybridization kinetics. *Biochemistry* 31:12055–12061.
2. Stull, R.A., Zon, G., and Szoka, F.C. Jr. 1996. An in vitro messenger RNA binding assay as a tool for identifying hybridization-competent antisense oligonucleotides. *Antisense & Nucleic Acid Drug Development* 6:221–228.
3. Peyman, A., Helsberg, M., Kretzschmar, G., Mag, M., Grabley, S. and Uhlmann, E. 1995. Inhibition of viral growth by antisense oligonucleotides directed against the IE110 and the UL30 mRNA of Herpes Simplex Virus type-1. *Biol. Chem. Hoppe-Seyler* 376:195–198.
4. Cazenave, C., Loreau, N., Toulmé, J.-J., and Hélène, C. 1986. Anti-messenger oligodeoxynucleotides: specific inhibition of rabbit β-globin synthesis in wheat germ extract and *Xenopus* oocytes. *Biochimie* 68:1063–1069.
5. Kozak, M. 1994. Features in the 5' non-coding sequences of Rabbit α and β-globin mRNAs that affect translational efficiency. *J. Mol. Biol.* 235:95–110.
6. Blake, K.R., Murakami, A., and Miller, P.S. 1988. Inhibition of rabbit globin mRNA translation by sequence-specific oligodeoxyribonucleotides. *Biochemistry* 24:6132–6138.
7. Cazenave, C., Loreau, N., Thoung, N.G., Toulmé, J.-J., and Hélène, C. 1987. Enzymatic amplification of translation inhibition of rabbit β-globin mRNA by anti-messenger oligodeoxynucleotides covalently linked to intercalating agents. *Nuc. Acids. Res.* 15:4717–4736.
8. Ratmeyer, L., Vinayak, R., Zhong, Y.Y., Zon, G., and Wilson, W.D. 1994. Sequence specific thermodynamic and structural properties for DNA RNA duplexes. *Biochemistry* 33:5298–5304.
9. Monia, B.P., Johnston, J.F., Geiger, T., Muller, M., and Fabbro, D. 1996. Antitumor activity of a phosphorothioate antisense oligodeoxynucleotide targeted against C-*raf* Kinase. *Nature Medicine* 2:668–675.
10. Stull, R.A., Taylor, L.A., and Szoka, F.C. Jr. 1992. Predicting antisense oligonucleotide inhibitory efficacy: a computational approach using histograms and thermodynamic indices. *Nuc. Acids. Res.* 20:3501–3508.
11. Thompson, S., Wolfscheid, V., Griffin, P., Salter, H., Sczakiel, G., and James, W. 1996. The role of long antisense arms in the activity of ribozymes against HIV-1: entrapping distal regions favorable for hybridization. *Nuc. Acids. Res.* Submitted.
12. Ho, S.P., Britton, D.H.O., Stone, B.A., Behrens, D.L., Leffet, L.M., Hobbs, F.W., et al. 1996. Potent antisense oligonucleotides to the human multidrug resistance-1 mRNA are rationally selected by mapping RNA-accessible sites with oligonucleotide libraries. *Nuc. Acids. Res.* 24:1901–1907.
13. Lima, W.F., Brown-Driver, V., Fox, M., Hanecak, R., and Bruice, T.W. 1997. Combinatorial screening and rational optimization for hybridization to folded Hepatitis C virus RNA of oligonucleotides with biological antisense activity. *J. Biol. Chem.* 272:626–638.
14. Wagner, R.W., Matteucci, M.D., Grant, D., Huang, T., and Froehler, B.C. 1996. Potent and selective inhibition of gene expression by an antisense heptanucleotide. *Nature Biotechnology* 14:840–844.
15. Southern, E.M., Case-Green, S.C., Elder, J.K., Johnson, M., Mir, K.U., Wang, L., and Williams, J.C. 1994. Arrays of complementary oligonucleotides for analysing the hybridization behavior of nucleic acids. *Nuc. Acids. Res.* 22:1368–1373.
16. Maskos, U. and Southern, E.M. 1992. Oligonucleotide hybridizations on glass supports: a novel linker for oligonucleotide synthesis and hybridisation properties of oligonucleotides synthesized in situ. *Nuc. Acids. Res.* 20:1679–1684.
17. Maniatis, T., Fritsch, E.F., and Sambrook, J. 1982. pp. 14.18–14.21 in *Molecular cloning, a laboratory manual*. Cold Spring Harbor Laboratory, Cold Spring Harbor, NY.
18. Rovera, G., Magarian, C., and Borun, T.W. 1978. Resolution of hemoglobin subunits by electrophoresis in acid urea polyacrylamide gels containing Triton X-100. Anal. Biochem 85:506–518.
19. Cazenave, C., Stein, C.A., Loreau, N., Thoung, N.G., Neckers, L.M., Subasinghe, C., et al. 1989. Comparative inhibition of rabbit globin mRNA translation by modified antisense oligodeoxynucleotides. Nuc. Acids. Res. 17:4255–4273.
20. Jaeger, J.A., Turner, D.H., and Zuker, M. 1989. Improved predictions of secondary structures for RNA. Proc. Natl. Acad. Sci. USA 86:7706–7710.

APPENDIX C

Antisense DNAs as multisite genomic modulators identified by DNA microarray

Yee Sook Cho*, Meyoung-Kon Kim*, Chris Cheadle†, Catherine Neary*, Kevin G. Becker†, and Yoon S. Cho-Chung*‡

*Cellular Biochemistry Section, Laboratory of Tumor Immunology and Biology, National Cancer Institute, National Institutes of Health, Bethesda, MD 20892-1750; and †DNA Array Unit, National Institute on Aging, National Institutes of Health, Baltimore, MD 21224-6820

Communicated by Paul C. Zamecnik, Massachusetts General Hospital, Charlestown, MA, June 21, 2001 (received for review May 4, 2001)

Antisense oligodeoxynucleotides can selectively block disease-causing genes, and cancer genes have been chosen as potential targets for antisense drugs to treat cancer. However, nonspecific side effects have clouded the true antisense mechanism of action and hampered clinical development of antisense therapeutics. Using DNA microarrays, we have conducted a systematic characterization of gene expression in cells exposed to antisense, either exogenously or endogenously. Here, we show that in a sequence-specific manner, antisense targeted to protein kinase A RIα alters expression of the clusters of coordinately expressed genes at a specific stage of cell growth, differentiation, and activation. The genes that define the proliferation-transformation signature are down-regulated, whereas those that define the differentiation-reverse transformation signature are up-regulated in antisense-treated cancer cells and tumors, but not in host livers. In this differentiation signature, the genes showing the highest induction include genes for the G proteins Rap1 and Cdc42. The expression signature induced by the exogenously supplied antisense oligodeoxynucleotide overlaps strikingly with that induced by endogenous antisense gene overexpression. Defining antisense DNAs on the basis of their effects on global gene expression can lead to identification of clinically relevant antisense therapeutics and can identify which molecular and cellular events might be important in complex biological processes, such as cell growth and differentiation.

The two isoforms of cAMP-dependent protein kinase (PKA), PKA-I and PKA-II, share a common catalytic subunit but contain distinct regulatory (R) subunits, RI and RII, respectively (1). Four different R subunits—RIα, RIβ, RIIα, and RIIβ—have been identified. Expression of the RIα subunit of PKA is increased in various human tumors and cell lines, including cancers of the breast (2–5), ovary (6, 7), lung (8), and colon (9–11). Furthermore, overexpression of the RIα subunit of PKA correlates with malignancy and poor prognosis in cancer patients (3–7). Therefore, the RIα subunit of PKA is a potential target for human cancer therapy. In the last decade, there have been increasing efforts to develop PKA-specific inhibitors as cancer therapeutic agents (12–19).

In the present study, we have investigated the sequence-specific effects of RIα antisense on global gene expression by using DNA microarray. We have used distinct antisense phosphorothioate oligonucleotides (PS-ODNs) targeted to the human RIα gene and the second-generation antisense ODN, which is a 2′-*O*-methyl RNA/DNA hybrid (19). We also examined the expression profile in cells endogenously overexpressing the RIα antisense gene. This system avoids the problems inherent in ODN treatment, namely, the delivery and stability of the ODN.

Methods

ODN Treatment. RIα antisense ODNs used were PS-ODN (15), RNA/DNA ODN (19), mouse PS-ODN (15), and appropriate control ODNs (15, 19). Cells were treated with antisense/control ODNs (0.2 μM, 3 days) by using the cationic liposomal transfection reagent DOTAP (*N*-[1-(2,3-dioleoyloxy)propyl]-*N*,*N*,*N*-trimethylammonium methylsulfate) (Roche Diagnostics).

RIα Antisense Gene Overexpression. Cells overexpressing the RIα antisense gene were generated by stable transfection with the RIα antisense gene [N-terminal 200 nt ligated into the OT1529 vector (20) (L. Tan and Y.S.C.-C., unpublished work)] and treatment with $ZnSO_4$ (60 μM, 3 days).

RNA Preparation. Total cellular RNA was prepared from control and antisense-exposed cells by using a RNeasy Midi Kit (Qiagen, Chatsworth, CA), electrophoresed, blotted onto nylon membrane, and subjected to Northern blot analysis (20). The specific fragments of cDNA corresponding to respective genes were generated by PCR.

cDNA Microarray Analysis. Total RNA prepared from the antisense-exposed and control cells were used to synthesize ^{33}P-labeled cDNAs by reverse transcription. The cDNAs were hybridized to a human cDNA microarray (2,304 elements) that was primarily derived from IMAGE consortium cDNA libraries (Research Genetics, Huntsville, AL), as described (21). Cluster analysis was performed on Z-transformed microarray data by using two separate programs available as shareware from Michael Eisen's laboratory (http://rana.lbl.gov).

Tumor Growth and Antisense Treatment. PC3 M cells (2×10^6 cells) were inoculated s.c. into nude mice. When tumors became palpable (30–50 mg), antisense or control ODN (0.1 mg/0.1 ml saline per mouse, daily) or saline (0.1 ml per mouse) was injected i.p. into the mice (16). After 4 days of treatment, animals were killed, and tumors, livers, and spleens were removed, weighed, immediately frozen in liquid N_2, and kept frozen at −80°C until used.

Results and Discussion

Parallel Expression Profiles Between Antisense ODN-Treated Cells and Cells Overexpressing the Antisense Gene. We hypothesized that the sequence-specific effects as well as various unexpected effects of antisense might reflect previously unrecognized gene expression patterns in treated cells. We thus used DNA microarray technology (22) to identify the sequence-specific mechanism for antisense RIα action. We used a cDNA microarray containing 2,304 nonredundant clones to analyze gene expression patterns in cells treated with RIα antisense RNA/DNA mixed backbone (19) ODN. Total RNA prepared from antisense-treated and untreated control cells was used to synthesize ^{33}P-labeled cDNAs, which were hybridized to cDNA microarray. Treatment of PC3 M prostate carcinoma cells with 0.2 μM RIα antisense for 3 days inhibited growth by 50%. We compared the expression

Abbreviations: PKA, cAMP-dependent protein kinase; ODN, oligonucleotide; PS-ODN, phosphorothioate ODN.

‡To whom reprint requests should be addressed at: National Cancer Institute, Building 10, Room 5B05, 9000 Rockville Pike, Bethesda, MD 20892-1750. E-mail: chochung@helix.nih.gov.

The publication costs of this article were defrayed in part by page charge payment. This article must therefore be hereby marked "*advertisement*" in accordance with 18 U.S.C. §1734 solely to indicate this fact.

Table 1. Expression profile of genes altered in PC3M cells treated with antisense ODN or overexpressing antisense gene

Genes	Fold change	
	AS ODN	AS gene
CDC42	20.0	18.9
Myosin light chain, alkali	14.4	14.0
Kinesin heavy chain	12.7	11.1
Endothelin-converting enzyme 1	12.5	10.0
CDC27	9.7	9.2
Lysosome-associated membrane protein 1	7.9	6.4
Basic transcription factor 3	6.9	8.8
RAP1A	5.4	6.3
Ras-related protein RA8-8	5.2	5.8
IL-3 receptor, α	4.7	3.6
MHC class II	4.4	4.2
Signal recognition particle receptor	3.8	3.4
Probable G protein-coupled receptor HM74	3.7	4.0
Integrin, α-6	3.6	3.7
PDE48, cAMP specific	2.3	3.2
Heat shock protein HSPA2	−2.3	−2.3
Transformation-sens. prot. IEF SSP 3521	−2.3	−2.9
Superoxide dismutase 1 (Cu/Zn)	−2.6	−2.6
Plasminogen-like protein	−2.7	−2.6
Mitogen-act. prot. kinase kinase kinase 5	−2.9	−2.8
Phosphatidylinositol 3-kinase associated p85	−3.1	−3.6
YY1 transcription factor	−3.2	−3.2
Cytochrome p450 IIE1	−3.7	−4.3
Natural killer cell protein 4	−4.0	−4.0
Collagen, type IV, alpha-4	−4.0	−4.5
Diacylglycerol kinase, γ (90 kDa)	−4.5	−4.5
Catalase	−6.7	−6.7
Ligase 1, DNA, ATP-dependent	−6.7	−6.7
M-phase inducer phosphatase 2	−7.7	−7.7
Crystallin Mu	−20.0	−20.0

AS ODN, antisense ODN treatment; AS gene, antisense gene overexpression. Fold change represents altered levels of expression in antisense ODN/antisense gene cells as compared to control cells.

profile induced by exogenous antisense ODN treatment with that induced by the endogenous antisense gene overexpression. To address the question of cell specificity, we also analyzed the expression profiles of LS-174T colon carcinoma cells transfected with the RIα antisense gene.

The expression levels of ≈240 cDNAs, representing 10% of the total DNA elements on the array, were altered (≥ 2-fold up-regulated or down-regulated) in antisense ODN or antisense gene-treated cells. The changes ranged from −20-fold to +27-fold (Table 1). In contrast, cells treated with the cationic lipid DOTAP (*N*-[1-(2,3-dioleoyloxy)propyl]-*N*,*N*,*N*-trimethylammonium methylsulfate) alone or DOTAP plus control ODN exhibited a minimal (< ±30% change) alteration in the expression profile, and the pattern of altered expression did not mimic that caused by antisense ODN treatment (data not shown).

The expression profile of cells treated with antisense ODN (Figs. 1*A* and 2*A*) exhibited striking overlaps with that of cells that overexpressed the antisense gene (Figs. 1*B* and 2*B*). The same cDNA elements that were up-regulated or down-regulated in antisense ODN-treated cells were similarly up-regulated or down-regulated in the cells overexpressing antisense gene (Table 1). Less than 2% of the altered expression profiles were specific to either antisense ODN-treated cells or cells overexpressing the antisense gene (Fig. 2*C*). These results indicate that antisense ODN treatment and endogenous antisense gene overexpression affected nearly identical genomic pathways. Furthermore, the antisense-induced alteration in the expression profile of PC3 M

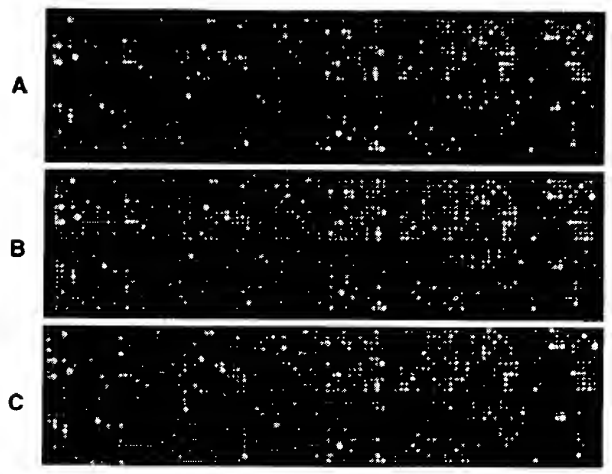

Fig. 1. Scanned phosphorimages of cDNA microarrays from RIα antisense ODN-treated cells and cells overexpressing the antisense gene, superimposed with images of respective control cells. (*A*) Antisense ODN-treated PC3 M cells. (*B*) Antisense gene overexpressing PC3 M cells. (*C*) LS-174T cells overexpressing the antisense gene. Genes up-regulated, compared with the control, are shown in red; down-regulated genes are shown in green, and yellow represents genes without changes in expression. The data represent one of four separate hybridizations that gave similar results.

cells was closely comparable to that of LS-174T cells overexpressing the antisense gene (Figs. 1 *B* and *C* and 2*F*), although the two cell lines exhibited large differences in their basic patterns of expression (Fig. 2*D*) and in the magnitude of altered expression (compare Fig. 2*B* with Fig. 2*E*). Thus, different cell types exhibit comparable expression profiles when treated with RIα antisense.

Northern Blotting Verifies Altered Gene Expression of Microarray. Northern blotting confirmed the microarray data, with changes in the expression profile exerted by the antisense ODN and antisense gene (that is, the direction of changes as well as the magnitude of altered expression) (Fig. 3). The Northern results further confirmed that the antisense RIα specifically down-regulated PKA RIα mRNA without affecting the expression of other PKA subunits (Fig. 3).

Molecular Portrait of Reverted Phenotype of Prostate Carcinoma. In addition to growth inhibition, RIα antisense treatment also induced changes in cell morphology, including a flat phenotype similar to the reverted phenotype of transformed cells (23). To obtain a molecular portrait of the "reverted" phenotype, we used a hierarchical clustering algorithm to group genes on the basis of similarity in their expression patterns (24). The data are presented in a matrix format (Fig. 4). Each row represents all of the hybridization results for a single DNA element of the array, and each column represents the expression levels for all genes in a single hybridization sample. The expression level of each gene is visualized, in color, relative to its median expression level across all samples. Red represents expression greater than the mean, and green represents expression less than the mean, and the intensity of the color denotes the degree of deviation from the mean (24). Distinct samples representing similar gene patterns from control cells were aligned in adjacent rows. Likewise, different samples from antisense ODN-treated or antisense gene-transfected cells were clustered in adjacent rows in our map. Also included in this map were samples from antisense-treated tumors, host livers, and various controls. The observed patterns of gene expression would thus reflect intrinsic differ-

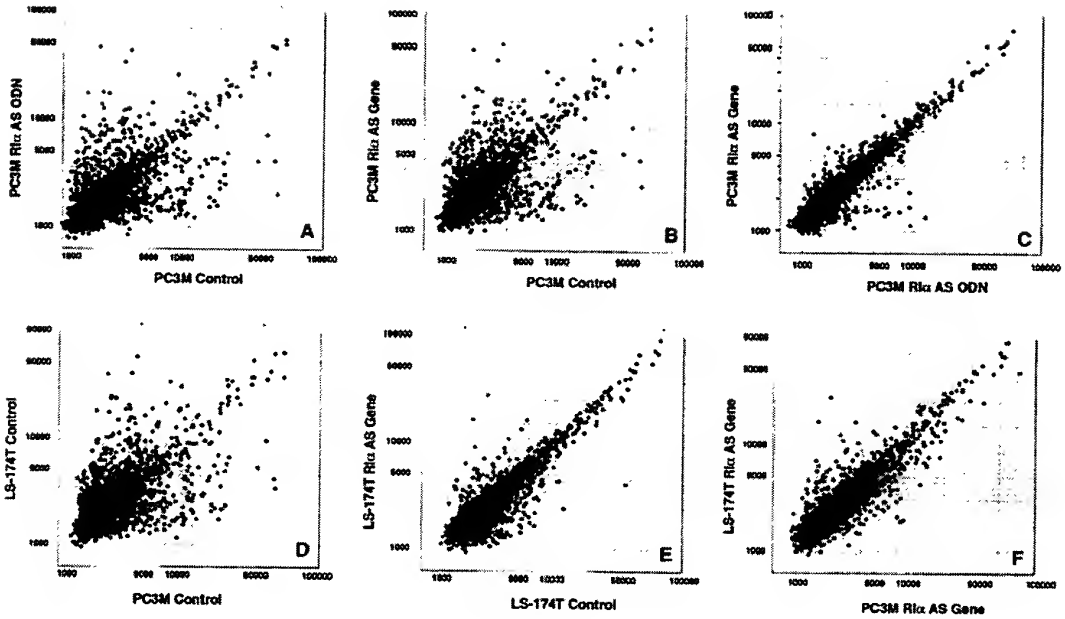

Fig. 2. Scatter plots for expression profile comparison between antisense ODN treatment and antisense gene overexpression and between PC3 M cells and LS-174T cells. Expression profiles of untreated control versus antisense (AS) ODN/gene-targeted cells (*A*, *B*, and *E*), AS ODN versus AS gene treatment (*C*), PC3 M control cells versus LS-174T control cells (*D*), and PC3 M cells overexpressing the antisense gene versus LS-174T overexpressing the antisense gene (*F*) are shown as bivariate scatterplots of 2,304 genes from the microarray. The values are corrected intensities representing levels of expression for the DNA elements of the microarrays (21).

ences between antisense-exposed cells and control cells rather than variations arising from experimental artifacts. We defined clusters of coordinately expressed genes as "signatures," which we named on the basis of the cellular process in which the component genes participate (25).

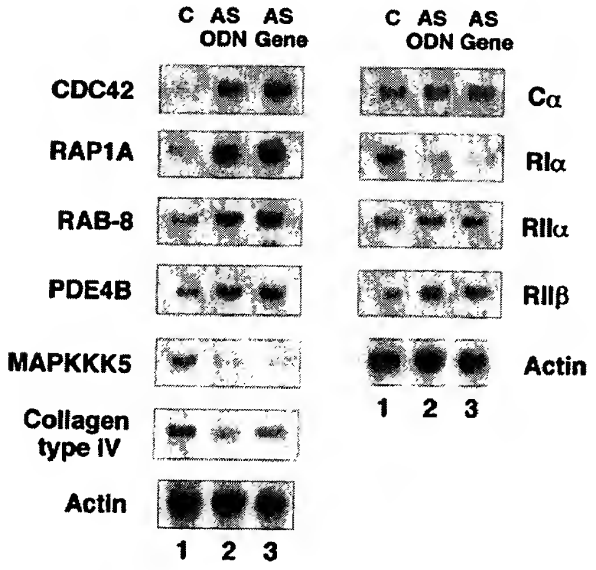

Fig. 3. Northern analysis of genes altered in PC3 M cells treated with antisense ODN or cells overexpressing antisense gene. C, untreated control cells; AS ODN, antisense ODN treatment; AS gene, antisense gene overexpression. The data represent one of two independent experiments that gave similar results.

Our map revealed that RIα antisense treatment affected a cluster of genes involved in proliferation and one involved in differentiation (Fig. 4). Genes that define the proliferation signature were highly expressed in untreated control cells (Fig. 4*E*, columns 1 and 2) and markedly suppressed in antisense-treated or -transfected cells (Fig. 4*E*, *Top* and *Middle*, columns 3–6). In this proliferation signature, genes encoding proteins involved in cell cycle control, DNA synthesis and regulation, transcription, and translation were predominant. Conversely, RIα antisense treatment induced genes involved in differentiation and reverse transformation (Fig. 4*D*). This cluster was dominated by genes encoding small G proteins, such as Cdc42 and Rap1, genes encoding transcription factors, and genes encoding regulatory proteins of the cytoskeleton, specifically the microtubules. Remarkably, the effects of RIα antisense treatment on these signatures were mirrored in cells overexpressing the antisense gene (Fig. 4, compare columns 3 and 4 with 5 and 6). The altered expression signatures generated by the RIα antisense ODN thus reflected true antisense effects rather than nonspecific antisense ODN effects described elsewhere (26).

Similar proliferation and differentiation signatures were observed in antisense-treated tumors (Fig. 4 *D* and *E*, *Top* and *Middle*, columns 10–12). However, we also observed an expression profile distinct from that observed in antisense-treated cells. For example, genes in the tumor-specific proliferation signature, such as those for TXK tyrosine kinase and Grb-2-associated protein, were markedly down-regulated in tumors, but unchanged in cells (Fig. 4*E* *Bottom*). Conversely, genes in the tumor-specific differentiation signature, such as those for developmental proteins, including wingless-type mouse mammary tumor virus integration site family and sex-determining region Y were markedly up-regulated in tumors, but not in cells (Fig. 4, legend). Likewise, genes in the transformation signature, such as oncogenes and genes for tyrosine and serine/threonine kinases that are usually overexpressed in tumors, were specifically

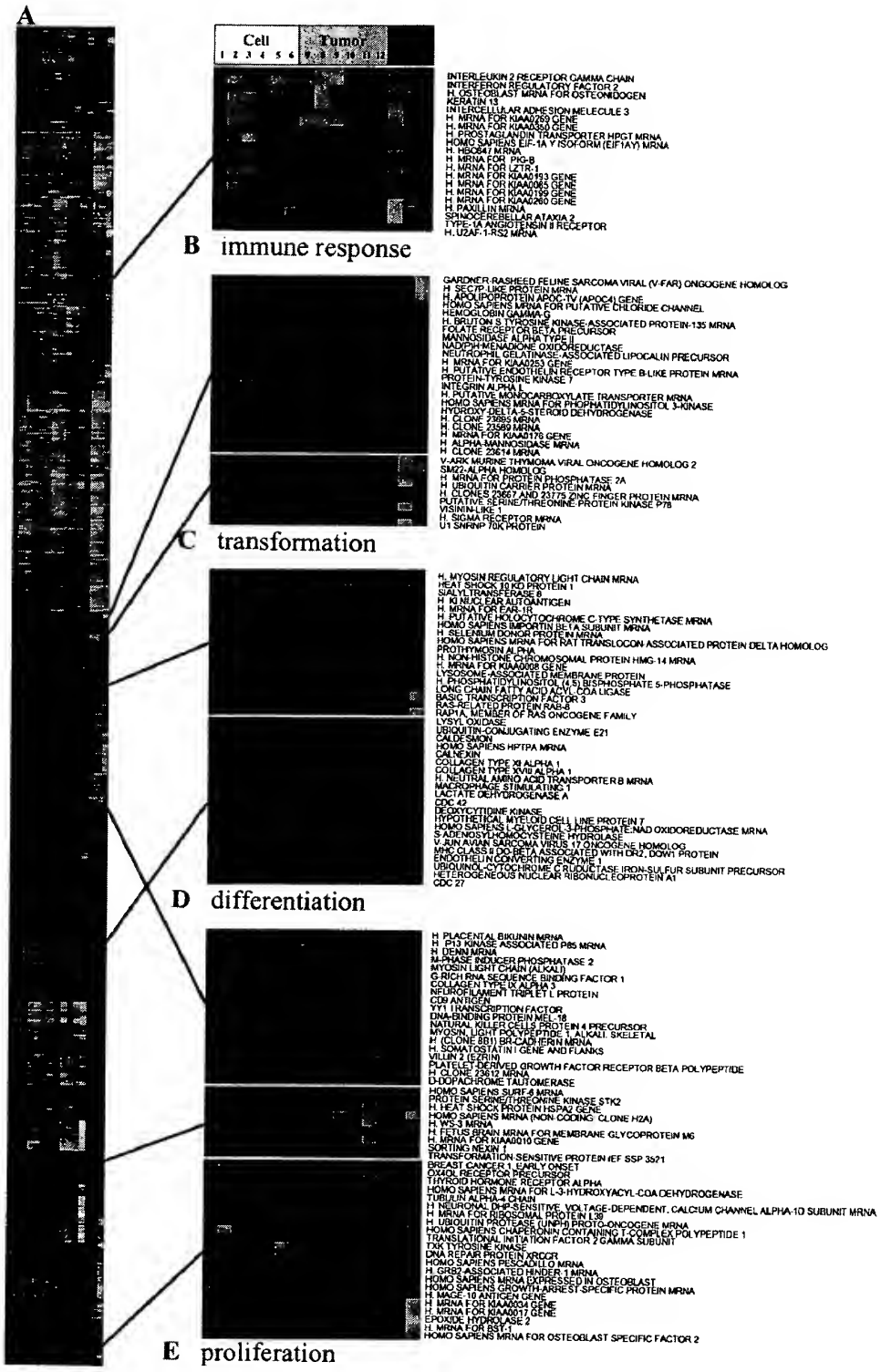

Fig. 4. Molecular portrait of the reverted phenotype of PC3 M cells and tumors treated with antisense RIα. Data from control ODN-treated cells, antisense ODN/gene-treated cells, untreated control cells, antisense ODN- or control ODN-treated tumors, control tumors, and host livers were combined and clustered. Cluster analysis was performed on Z-transformed microarray data by using two separate programs available as shareware from Michael Eisen's lab (http://rana.lbl.gov). Each gene is represented by a single row of colored boxes; each experimental sample is represented by a single column. Columns 1 and 2, untreated control cells. Columns 3 and 4, antisense RNA/DNA hybrid ODN-treated cells. Columns 5 and 6, antisense gene overexpressing cells. Columns 7 and 8, untreated control tumors. Column 9, control ODN-treated tumor. Column 10, antisense RNA/DNA ODN-treated tumor. Column 11, mouse antisense PS-ODN-treated tumor. Column 12, antisense PS-ODN-treated tumor. Column 13, antisense PS-ODN-treated liver. Column 14, antisense RNA/DNA ODN-treated liver. Column 15, untreated control liver. The entire clustered image is shown in *A*. Full gene names are shown for representative clusters containing functionally related genes involved in (*B*) immune response, (*C*) transformation, (*D*) differentiation, and (*E*) proliferation. These clusters also contain uncharacterized genes and named genes not involved in these processes. The up-regulation of Cdc42 in tumors is not apparent in *D* because of its high basal levels. The deviations of log ratios of expression levels from controls in antisense ODN-treated cells and tumors were 4.77 and 1.84, respectively. The expression levels of genes for the wingless-type mouse mammary tumor virus integration site family and sex-determining region Y were not depicted in *D*. The deviations of log ratios of these genes from controls were 0.26 and 1.08, respectively, in antisense-treated cells and 1.90 and 2.04, respectively, in antisense-treated tumors. The size of the tumors compared with untreated (saline injected) control tumors were: 42%, 63%, 56%, and 98%, after 4 days of treatment with antisense RNA/DNA ODN, PS-ODN, mouse PS-ODN, and control ODN, respectively. There was no sign of systemic toxicity in treated animals, and the size of the liver and spleen remained unchanged.

down-regulated in tumors only, but not in cells, after antisense treatment (Fig. 4*C*).

To verify the specificity of the antisense effects on gene expression signatures, we used three different antisense ODNs that differed in sequence or chemical modification: a PS-ODN antisense (15), directed against codons 8–13 of human RIα; the immunosuppressive (27), less cytotoxic (18), second-generation RNA/DNA hybrid PS-ODN antisense (19); and a nonimmunostimula-

tory 5′-CCG-containing (28) PS-ODN antisense (15), targeted to codons 8–13 of mouse RIα, that can cross hybridize with human RIα. The immune-response signature elicited in the PS-ODN antisense-treated tumors was undetectable in the RNA/DNA hybrid antisense-treated tumors (Fig. 4*B*, column 10). The expression signatures of mouse RIα antisense were in close parallel with that of the RNA/DNA hybrid antisense (Fig. 4, columns 10 and 11), without immunostimulatory effect (Fig. 4*B*, column 11). Overall, the alterations in expression signatures described above were similarly induced by all three antisense ODNs in tumors (Fig. 4, columns 10–12), but not in host livers (Fig. 4, columns 13 and 14). By contrast, the expression signatures of antisense were not elicited by control ODN (Fig. 4, column 9), indicating that antisense modulation of the expression signatures described above was sequence-specific. These expression signatures, together with other prominent features of the antisense-induced expression profile, appear to reflect the profile of the nonmalignant or reverted phenotype, which was shared by that observed in the host livers examined.

Conclusions

Antisense technology has been applied to specifically block disease-causing genes (29, 30); therefore, its use as a gene-specific therapeutic agent is highly promising. Targeting of cancer genes by antisense ODNs could inhibit tumor growth. However, nonspecific side effects caused by antisense ODNs (26) have clouded the understanding of the single-gene targeting mechanism of action and hampered or delayed clinical development of antisense drugs. Our results have revealed a specific subset of genes in cancer cells that are coordinately regulated by antisense RIα in a sequence-specific manner. This study shows that a view of global gene expression in cancer cells exposed to antisense ODN can refine the antisense mechanism with respect to its sequence and target specificity.

Our results show that antisense acts as a multisite genomic modulator and thus goes beyond functioning as a single gene-targeting agent. RIα antisense, once in the cell, alters the expression of hundreds of different genes, including its own target gene, and these genes can be classified into subgroups, which pinpoint specific stages of cell growth, differentiation, and transformation. Importantly, the differentiation and proliferation expression signatures were altered specifically in tumor cells; these signatures were quiescent and unaltered in the host livers of antisense-treated animals.

In this differentiation signature, the genes showing the highest induction included genes for Rap1A and Cdc42, small G proteins with GTPase activity. Both Rap1A and Cdc42 are multifunctional proteins related to both cell proliferation and differentiation (31). However, the RIα antisense induction of these G proteins in cancer cells occurred concomitantly with the induction of other proteins involved in differentiation and with the down-regulation of a cluster of genes involved in cell proliferation and transformation. Thus, in this case, the induction of these G proteins appears to promote differentiation and reverse transformation rather than proliferation and transformation in cancer cells.

Although we know that RIα antisense behaves as a multisite genomic modulator, its precise molecular mechanism of action is still unknown. We speculate that cAMP response element-directed transcription (32), which is triggered by the activation of PKA via antisense depletion of RIα (19), may play a central role in this process.

Gene expression profiling presents a way of refining cancer chemotherapeutics in the future. Revisiting antisense-targeted gene expression on a genomic scale will facilitate the discovery of clinically appropriate antisense drugs as well as providing a unique perspective on the development of new chemotherapeutic combinations based on the molecular actions of these drugs.

We thank Dr. Sudhir Agrawal for providing ODNs. We also thank Dr. Frances McFarland of Palladian Partners, Inc., who provided editorial support under Contract NO2-BC-76212/C2700212 with the National Cancer Institute. The member who communicated this paper is on the Board of Directors of Hybridon, Inc., for which a patent related to RIα has been licensed.

1. McKnight, G. S., Clegg, C. H., Uhler, M. D., Chivia, J. C., Cadd, G. G., Correll, L. A. & Otten, A. D. (1988) *Recent Prog. Horm. Res.* **44,** 307–355.
2. Handschin, J. S. & Eppenberger, U. (1979) *FEBS Lett.* **106,** 301–304.
3. Miller, W. R., Hulme, M. J., Cho-Chung, Y. S. & Elton, R. A. (1993) *Eur. J. Cancer* **29,** 989–991.
4. Miller, W. R., Watson, D. M. A., Jack, W., Chetty, U. & Elton, R. A. (1993) *Breast Cancer Res. Treat.* **26,** 89–94.
5. Miller, W. R., Hulme, M. J., Bartlett, J. M., MacCallium, J. & Dixon, J. M. (1997) *Clin. Cancer Res.* **3,** 2399–2404.
6. Simpson, B. J. B., Ramage, A. D., Hulme, M. J., Burns, D. J., Katsaros, D., Langdon, S. P. & Miller, W. R. (1996) *Clin. Cancer Res.* **2,** 201–206.
7. McDaid, H. M., Cairns, M. T., Atkinson, R. I., McAleer, S., Harkin, D. P., Gilmore, P. & Johnston, P. G. (1999) *Br. J. Cancer* **79,** 933–939.
8. Young, M. R. I., Montpetit, M., Lozano, Y., Djordjevic, A., Devata, S., Matthews, J. P. & Yedavalli, S. (1995) *Int. J. Cancer* **61,** 104–109.
9. Bradbury, A. W., Carter, D. C., Miller, W. R., Cho-Chung, Y. S. & Clair, T. (1994) *Br. J. Cancer* **69,** 738–742.
10. Bold, R. J., Alpard, S., Ishizuka, J., Townsend, C. M., Jr. & Thompson, C. J. (1994) *Regul. Pept.* **53,** 61–70.
11. Gordge, P. C., Hulme, M. J., Clegg, R. A. & Miller, W. R. (1996) *Eur. J. Cancer* **32,** 2120–2126.
12. Cho-Chung, Y. S. (1990) *Cancer Res.* **50,** 7093–7100.
13. Tortora, G., Yokozaki, H., Pepe, S., Clair, T. & Cho-Chung, Y. S. (1991) *Proc. Natl. Acad. Sci. USA* **88,** 2011–2015.
14. Rohlff, C. & Glazer, R. I. (1995) *Cell. Signalling* **7,** 431–443.
15. Nesterova, M. V. & Cho-Chung, Y. S. (1995) *Nat. Med.* **1,** 528–633.
16. Cho-Chung, Y. S., Nesterova, M., Kondrashin, A., Noguchi, K., Srivastava, R. & Pepe, S. (1997) *Antisense Nucleic Acid Drug Dev.* **7,** 217–223.
17. Wang, H., Cai, Q., Zeng, X., Yu, D., Agrawal, S. & Zhang, M. Q. (1999) *Proc. Natl. Acad. Sci. USA* **96,** 13989–13994.
18. Chen, H. X., Marshall, J. L., Ness, E., Martin, R. R., Dvorchik, B., Rizvi, N., Marquis, J., McKinlay, M., Dahut, W. & Hawkins, M. J. (2000) *Clin. Cancer Res.* **6,** 1259–1266.
19. Nesterova, M. V. & Cho-Chung, Y. S. (2000) *Antisense Nucleic Acid Drug Dev.* **10,** 423–433.
20. Nesterova, M., Yokozaki, H., McDuffie, L. & Cho-Chung, Y. S. (1996) *Eur. J. Cancer* **253,** 486–494.
21. Tanaka, T. S., Jaradat, S. A., Lim, M., Kargul, G. J., Wang, X., Grahovac, M. J., Pantano, S., Sano, Y., Piao, Y., Nagaraja, R., *et al.* (2000) *Proc. Natl. Acad. Sci. USA* **97,** 9127–9132.
22. Schena, M., Shalon, D., Davis, R. W. & Brown, P. O. (1995) *Science* **270,** 467–470.
23. Noda, M., Ko, M., Ogura, A., Liu, D. G., Amano, T., Takano, T. & Ikawa, Y. (1985) *Nature (London)* **318,** 73–75.
24. Eisen, M. B., Spellman, P. T., Brown, P. O. & Botstein, D. (1998) *Proc. Natl. Acad. Sci. USA* **95,** 14863–14868.
25. Alizadeh, A. A., Eisen, M. B., Davis, R. E., Ma, C., Lossos, I. S., Rosenwald, A., Boldrick, J. C., Sabet, H., Tran, T., Yu, X., *et al.* (2000) *Nature (London)* **403,** 503–511.
26. Stein, C. A. (1995) *Nat. Med.* **1,** 1119–1121.
27. Zhao, Q., Yu, D. & Agrawal, S. (1999) *Bioorg. Med. Chem. Lett.* **9,** 3453–3458.
28. Krieg, A. M., Yi, A. K., Matson, S., Waldschmidt, T. J., Bishop, G. A., Teasdale, R., Koretzky, G. A. & Klinman, D. M. (1995) *Nature (London)* **374,** 546–549.
29. Zamecnik, P. & Stephenson, M. (1978) *Proc. Natl. Acad. Sci. USA* **75,** 280–284.
30. Cho-Chung, Y. S. (2000) *Exp. Opin. Ther. Patents* **10,** 1711–1724.
31. Hall, A. (1994) *Annu. Rev. Cell Biol.* **10,** 31–54.
32. Roesler, W. J., Vandenbark, G. R. & Hanson, R. W. (1988) *J. Biol. Chem.* **263,** 9063–9066.